DUDLEY KNOX LIBRARY
NAVAL POSTGRADUATE SCHOOL
MONTEREY, CALIFORNIA 93943-5002

NAVAL POSTGRADUATE SCHOOL
Monterey, California

THESIS

L43565

DIFFRACTION TRANSITION RADIATION FROM PERIODIC ELECTRON BUNCHES

by

Lee, Young Moon

December 1987

Thesis Advisor: Fred R. Buskirk

Approved for public release; distribution is unlimited

T239202

REPORT DOCUMENTATION PAGE

REPORT SECURITY CLASSIFICATION: Unclassified

1b RESTRICTIVE MARKINGS

SECURITY CLASSIFICATION AUTHORITY

3 DISTRIBUTION / AVAILABILITY OF REPORT: Approved for public release; distribution is unlimited

DECLASSIFICATION / DOWNGRADING SCHEDULE

ERFORMING ORGANIZATION REPORT NUMBER(S)

5 MONITORING ORGANIZATION REPORT NUMBER(S)

NAME OF PERFORMING ORGANIZATION: Naval Postgraduate School

6b OFFICE SYMBOL (If applicable): 61

7a NAME OF MONITORING ORGANIZATION: Naval Postgraduate School

ADDRESS (City, State, and ZIP Code): Monterey, California 93943-5000

7b ADDRESS (City, State, and ZIP Code): Monterey, California 93943-5000

NAME OF FUNDING / SPONSORING ORGANIZATION

8b OFFICE SYMBOL (If applicable)

9 PROCUREMENT INSTRUMENT IDENTIFICATION NUMBER

ADDRESS (City, State, and ZIP Code)

10 SOURCE OF FUNDING NUMBERS

PROGRAM ELEMENT NO	PROJECT NO.	TASK NO	WORK UNIT ACCESSION NO.

TITLE (Include Security Classification): Diffraction Transition Radiation from Periodic Electron Bunches

PERSONAL AUTHOR(S): Lee, Young Moon

TYPE OF REPORT: Master's Thesis

13b TIME COVERED: FROM ________ TO ______

14 DATE OF REPORT (Year, Month, Day): 1987 December

15 PAGE COUNT: 71

SUPPLEMENTARY NOTATION

COSATI CODES		
FIELD	GROUP	SUB-GROUP

18 SUBJECT TERMS (Continue on reverse if necessary and identify by block number): Diffraction transition radiation, Transition radiation, Cerenkov radiation, Normalization

ABSTRACT (Continue on reverse if necessary and identify by block number)

Measurements of the first lobe of diffraction transition radiation from a hole in a thin aluminum foil for electron-beam energies of 32.9 MeV and 63.3 MeV has been made. The effect of the hole size was investigated using radii of 3 cm, 5 cm, and 7 cm. Although the measured peak angle and intensity are not well matched to the theoretical values, these experiments attempt to isolate the diffraction transition radiation from Cerenkov radiation and transition radiation. The normalization of the detected signal to the beam current was tried for compensation of the beam fluctuation. Conclusive results have not yet been obtained, but this investigation provides directions for future experiments.

DISTRIBUTION / AVAILABILITY OF ABSTRACT: ☒ UNCLASSIFIED/UNLIMITED ☐ SAME AS RPT ☐ DTIC USERS

21 ABSTRACT SECURITY CLASSIFICATION: Unclassified

NAME OF RESPONSIBLE INDIVIDUAL: Professor Fred R. Buskirk

22b TELEPHONE (Include Area Code): (408) 646 - 2765

22c OFFICE SYMBOL: 61Bs

FORM 1473, 84 MAR

83 APR edition may be used until exhausted

All other editions are obsolete

SECURITY CLASSIFICATION OF THIS PAGE

Unclassified

☆ U.S. Government Printing Office: 1986—606-24.

Approved for public release; distribution is unlimited

Diffraction Transition Radiation
from Periodic Electron Bunches

by

Lee, Young Moon
Major, Republic of Korea Army
B.S. Korea Military Academy, 1976

Submitted in partial fulfillment of the
requirements for the degree of

MASTER OF SCIENCE IN PHYSICS

from the

NAVAL POSTGRADUATE SCHOOL
December 1987

ABSTRACT

Measurements of the first lobe of diffraction transition radiation from a hole in a thin aluminum foil for electron-beam energies of 32.9 MeV and 63.3 MeV has been made. The effect of the hole size was investigated using radii of 3 cm, 5 cm, and 7 cm. Although the measured peak angle and intensity are not well matched to the theoretical values, these experiments attempt to isolate the diffraction transition radiation from Cerenkov radiation and transition radiation. The normalization of the detected signal to the beam current was tried for compensation of the beam fluctuation. Conclusive results have not yet been obtained, but this investigation provides directions for future experiments.

Thesis
W3565
c.1

TABLE OF CONTENTS

I. INTRODUCTION 6
  A. BACKGROUND 6
  B. PREVIOUS INVESTIGATIONS 9
  C. CERENKOV RADIATION AND TRANSITION RADIATION . 11
  D. PURPOSE 16
II. THE EXPERIMENT 17
  A. EXPERIMENTAL SETUP 17
    1. The end station 18
    2. Control Room 22
  B. PROCEDURE 24
    1. Digitization 24
    2. Normalization 26
    3. Data collection 28
III. RESULTS AND CONCLUSIONS 38
  A. RESULTS 38
  B. CONCLUSIONS 58
APPENDIX A : LINAC CHARACTERISTICS 60
APPENDIX B : BASIC PROGRAM LISTINGS 61
LIST OF REFERENCES 67
INITIAL DISTRIBUTION LIST 68

DUDLEY KNOX LIBRARY
NAVAL POSTGRADUATE SCHOOL
[illegible]

ACKNOWLEDGEMENTS

I would like to express my gratitude and appreciation to Professor F. R. Buskirk and Professor X. K. Maruyama for their advice and guidance in all phases of this research.

Also, assistance of Mr. D. Snyder for the operation and maintenance of the NPS LINAC is greatly appreciated.

At the end, I am grateful to my wife, Kyoung Soon, for her understanding and support throughout this work and complete study at NPS.

This paper is dedicated to my children, Sang Hag and Sang Un.

Lee, Young Moon

I. INTRODUCTION

A. BACKGROUND

Diffraction Transition Radiation (DTR) occurs when a charged particle of constant velocity passes through a hole or near any interface between two media which posses different dielectric constants. For example, a related process occurs in linear accelerators, in which bunched charges lose energy in transiting the radio frequency accelerating modules and this effect is known as "beam loading" [Ref. 1].

A lot of research has been done on diffraction transition radiation which is usually associated with a single charged particle. Ter-Mikaelian discusses the fast charged particle passing through a circular hole [Ref. 2]. Since the fast particle field becomes equivalent to a set of plane waves, the calculation for diffraction problem is similar to a procedure for calculating the diffraction of light waves, as well as involving scattering based on the Huygens principle.

This approach is valid if the incident wavelength, λ (actually $\lambda/2$), on the hole is small compared to the radius, a, of the hole. In addition, deflection angles, θ, of the incident wave direction must be small. (That is, the laws of geometrical optics allow small deviations.) Also, a point charge is assumed. Therefore, the two following conditions should be satisfied

$$ƛ \ll a \qquad (1)$$

$$\theta \ll 1 \qquad (2)$$

While these condition should be maintained, Ter-Mikaelian considers the process of the scattering of pseudo-photons. Since the particle field for a fast particle depends on the distance from its path, the Fourier components of the particle are spatially limited in a cicle of the radius $a \sim ƛ\gamma$ [Ref.2]. Then the following condition should be fulfilled for the radiation of angular frequency, ω , to occur.

$$(ƛ / a) \geq \gamma^{-1} \qquad (3)$$

where γ is the Lorentz factor. The better the condition is fulfilled, the greater the radiated intensity.

When a charged particle which has a velocity v, passes through a hole of radius a, with a distance R, from the axis as in Figure 1 (Figure 10 [Ref. 1]). With the limits

$$\gamma v/\omega \gg a \quad \text{and} \quad R \ll a \qquad (4)$$

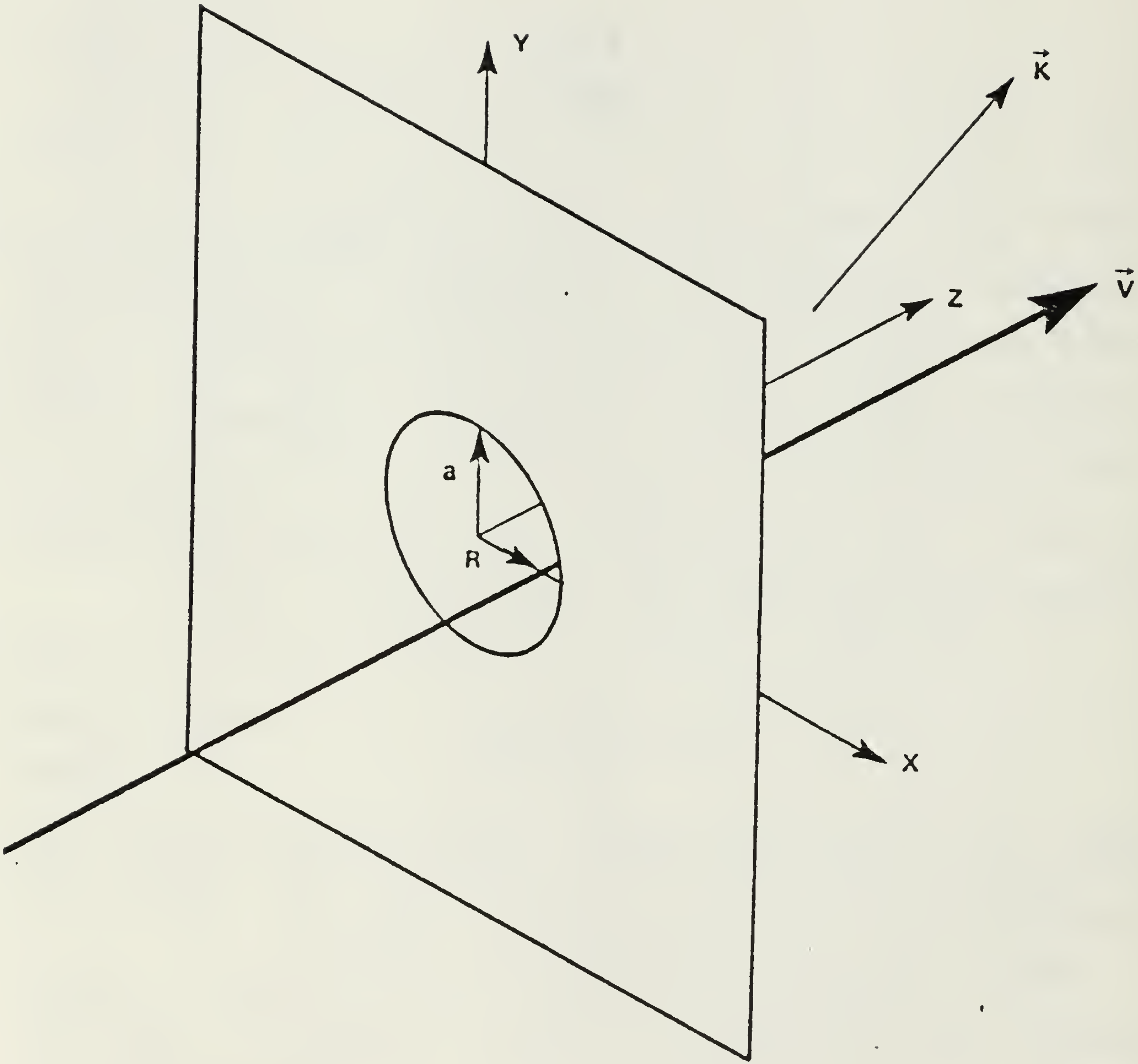

Figure 1. Diffraction Transition Radiation of wave vector k produced by a particle of velocity V transiting a distance R from the center of a hole of radius a in a screen.

Ter-Mikaelian developed an expression for the number of quanta of frequency, ω , radiated in the range of the angles $d\theta$ by one electron, given as [Ref. 2]

$$Nd\omega d\theta \approx \frac{1}{137}\,\frac{\theta^{3}d\theta}{(\gamma^{-2}+\theta^{2})^{2}}\left[J_{0}^{2}(qa)+\left(\frac{R}{a}\right)^{2}J_{1}^{2}(qa)\right]\frac{d\omega}{\omega} \qquad (5)$$

where the factor q in the argument of the Bessel functions $J_0(qa)$ and $J_1(qa)$ is the projection of the wave vector **k** into the plane z = 0 of Figure 1 ($q = k \sin\theta$). If R = 0 and equation (4) is satisfied, the electric field components are

$$E_x = \frac{ie}{2\,{}^{2}c}\,\frac{q}{q^{2}+\alpha^{2}}\,J_0(qa)\cos\phi \qquad (6)$$

$$E_y = \frac{ie}{2\,{}^{2}c}\,\frac{q}{q^{2}+\alpha^{2}}\,J_0(qa)\sin\phi \qquad (7)$$

where ϕ is the angle of **q** with respect to the x-axis and $\alpha = w/\gamma v$ [Ref. 2]. From equations (6) and (7), the radiation is polarized with the electric vector lying in the plane containing the vectors v and **k**.

B. PREVIOUS INVESTIGATIONS

Rule and Fiorito discuss that for development of diffraction transition radiation as a noninterceptive diagnostic it will be necessary to accurately measure the angular dependence of DTR spectrum in the submillimeter regime. Also they state that the coherent DTR should be produced if the separations of the beam particle are on the order of or smaller than a wavelength. Diffraction transition radiation will begin to be produced by the beam at wavelengths satisfying the relation [Ref. 1]

$$n_b^{-1/3} \leq \lambda \tag{8}$$

where n_b is the beam density. When this relation is strongly satisfied, both transition radiation (TR) and diffraction transition radiation will be enhanced and the intensity of the radiation will become proportional to n_b^2 rather than to n_b.

In 1986, O'Grady did an experiment to look at the diffraction transition radiation using a mirror in the beam path to reflect the radiation [Ref. 3]. A hole in a metal plate covers the beam tube exit window and varies its size. His results were the first experiment to produce DTR at Naval Postgraduate School Accelerator Laboratory (NPSAL). Data was taken at 3 different energies and compared with different sizes of holes and with no hole in a plate which generates TR. There were differences in the diffraction patterns which must be attributed to DTR.

In 1986, Gallet derived the equations regarding diffraction transition radiation from relativistic electron bunches passing through an aperture from the Huygens-Fraunhofer treatment of the fields across the aperture [Ref. 4]. These results come from the first theoretical approach to have considered the effects of electron bunching. The DTR pattern from a relativistic electron beam is very similar to the case of that in which a plane wave incident on a circular aperture results in the Airy diffraction pattern. It differs, however, from the optical diffraction pattern in that the central maximum is replaced by a null which results from the radial nature of the electron fields and strongly depends on aperture size. Increasing the aperture size, decreases the peak at $\theta = \gamma^{-1}$ and shifts the structure toward to the $\theta = 0$ axis. A strong peak is present at $\theta = \gamma^{-1}$ (which is characteristic of TR) and the strength of the peak is dependent on the energy of the beam.

C. CERENKOV RADIATION AND TRANSITION RADIATION

Diffraction transition radiation is closely related to TR which occurs when a charged particle of constant speed passes through a boundary where the dielectric constants of the medium change, and Cerenkov radiation which results when a charged particle moves through a transparent medium faster than the phase velocity of light in the medium.

Buskirk and Neighbours formulated the equation for the power of Cerenkov radiation from periodic electron bunches in 1982. This equation predicted the power from the harmonics of the fundamental period [Ref. 5]. In 1983, Buskirk and Neighbours calculated the diffraction effects in Cerenkov radiation produced by a finite path length. This relation for the diffracted power radiated in watts per steradian is [Ref. 6]

$$W(\nu, \tilde{n}) = \nu_0^2 \; Q \; R^2 \quad \text{(Watts/steradian)} \tag{9}$$

where $Q = \mu \, c \, q^2 \, / \, (8\pi)$

q = charge in electron bunch

ν_0 = fundamental frequency of the beam generator

$R = k \, L \sin\theta \; I(u) \; F(k)$

and where

$k = 2\pi / \lambda$: wave number of Cerenkov radiation

$= j \, k_0$: j = integer

k_0 = wave number for ν_0

L = finite interaction beam length

$I(u) = \sin(u) / u$: diffraction pattern

: $u = kL(\cos\theta_c - \cos\theta)/2$

$F(k)$ = form factor of the charge distribution bunch, considered unity when the bunch length is smaller than wavelength

$\cos\theta_c = c'/V = 1/(n\beta)$ = Cerenkov angle

θ = observation angle from the beam direction

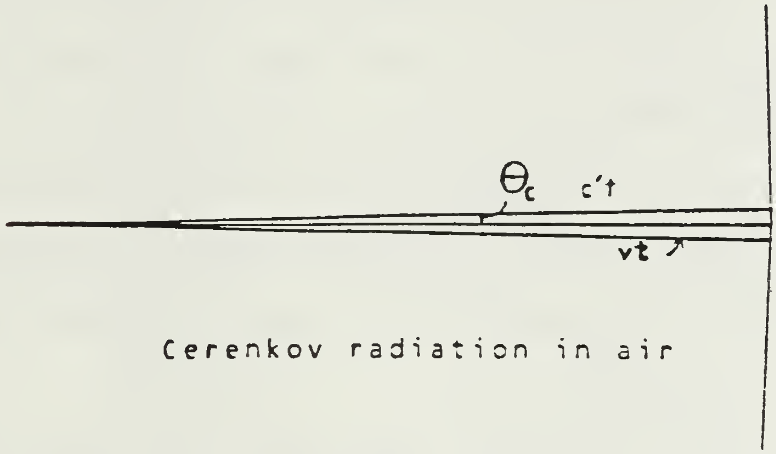

Cerenkov radiation in air

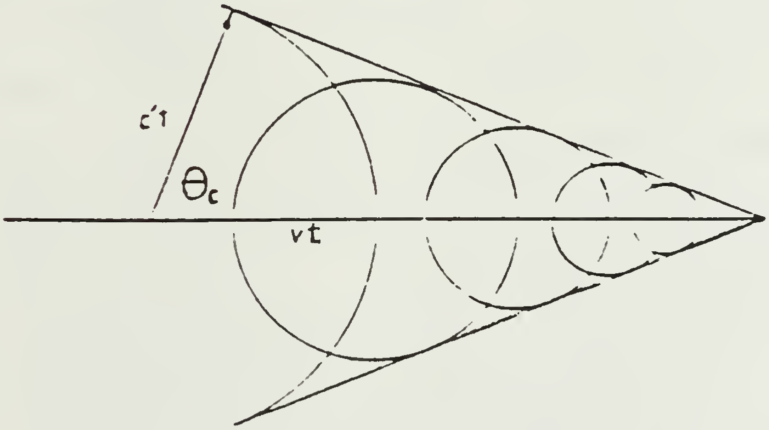

Idealized Cerenkov radiation in a medium with a high n

Figure 2. Cerenkov Radiation

From this equation, the peak of the power, for the case $L \gg \lambda$ occurs when $\theta = \theta_c$.

If a charged particle passes the boundary where the dielectric properties of the medium are different, then transition radiation will always be produced. Although TR is closely associated with Cerenkov radiation, the properties are quite different. The most important property is that the intensity of TR is strongly dependent on the energy of the charged particle [Ref. 1], whereas for Cerenkov radiation the intensity depends on the speed of the charged particle [Ref. 5].

The generated spectrum ranges from the microwave to the X-ray region, where the upper limit is proportional to the Lorentz factor γ. Transition radiation is also polarized and angularly dependent. For relativistic particles normally incident to the interface, the maximum intensity occurs at the angle [Ref. 1]

$$\theta_p \approx 1/\gamma \equiv mc^2/E \qquad (10)$$

where E is the total energy and mc^2 is the rest energy of the particle (Figure 3).

Cerenkov radiation, TR and DTR all occur when the charged particle is traveling at constant velocity through or near a medium. Cerenkov radiation has a velocity threshold such that the phase velocity of a particle is

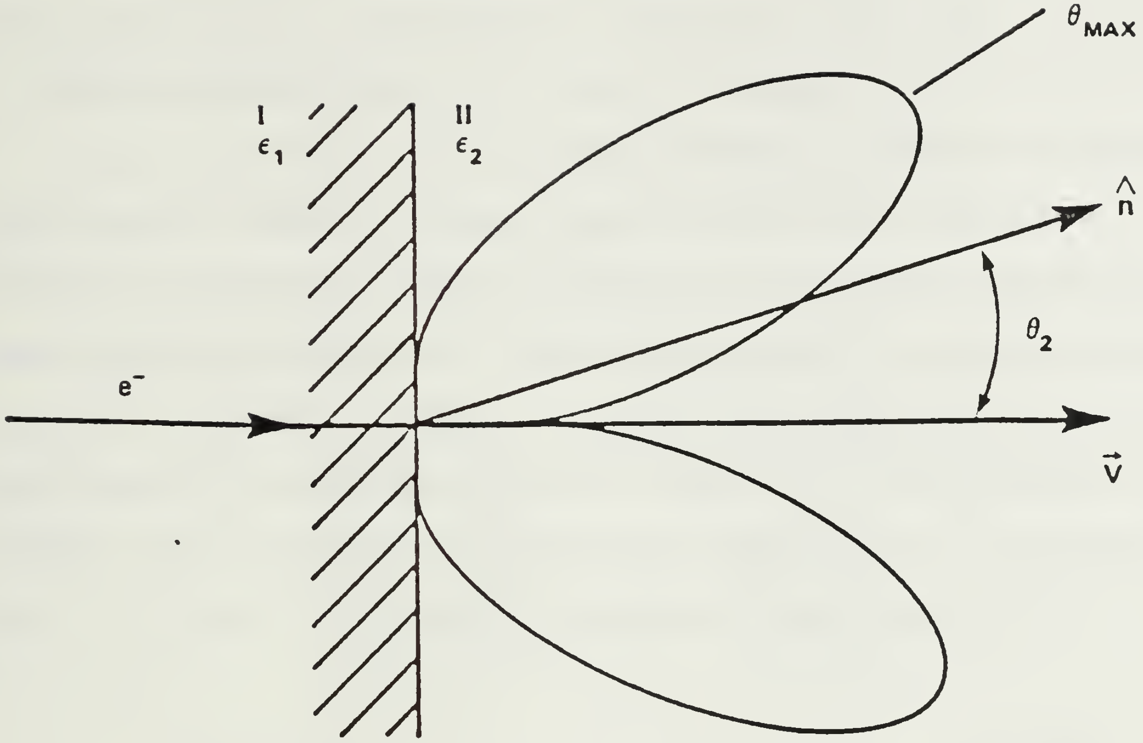

Notes : Medium I and medium II have dielectric functions ϵ_1 and ϵ_2. The direction of observation is n at an angle θ_2 with respect to the particle velocity V. Not shown is the backward TR which has a similar intensity distribution.

Figure 3. Transition radiation produced in the forward direction at an interface

faster than the light velocity in a medium. The Cerenkov angle θ_c is related to the index of refraction and the particle velocity as shown in Equation 9. TR and DTR intensities and angles of emission depend on the particle's energy as shown in Equation 10.

In case of NPSAL, the electron beam passes the accelerator beam pipe through a circular KAPTON aperture where transition and diffraction transition radiation may have been produced and enters air where Cerenkov radiation was produced. For a 50 MeV electron beam, the peak of intensity for Cerenkov radiation is about 1.19 degree (n=1.000268) and 0.59 degree for TR and DTR.

D. PURPOSE

This experiment is primarily focused on isolating diffraction transition radiation from the transition radiation and Cerenkov radiation to investigate closely the distribution of radiation intensity as a function of angle, hole size, and dependent on the beam energy.

A secondary focus is to improve the method of recording data. Previous work in NPSAL assume the beam density to be stable; however, the beam is unstable and sometimes goes to zero. Because the radiation field is dependent on the current, the observed field signal should be corrected when the beam changes. This correction is called normalization.

II. THE EXPERIMENT

A. EXPERIMENTAL SETUP

This experiment was performed using an electron linear accelerator (LINAC) at the Naval Postgraduate School. The experimental station and the characteristics of the LINAC is described in Appendix A. The experimental setup in the end station is shown in Figure 4, and is basically similar to that used by O'Grady [Ref. 3] and by Bruce [Ref. 7]. However, several new concepts and alternate equipments are used. A mirror is not used for direct measurement of

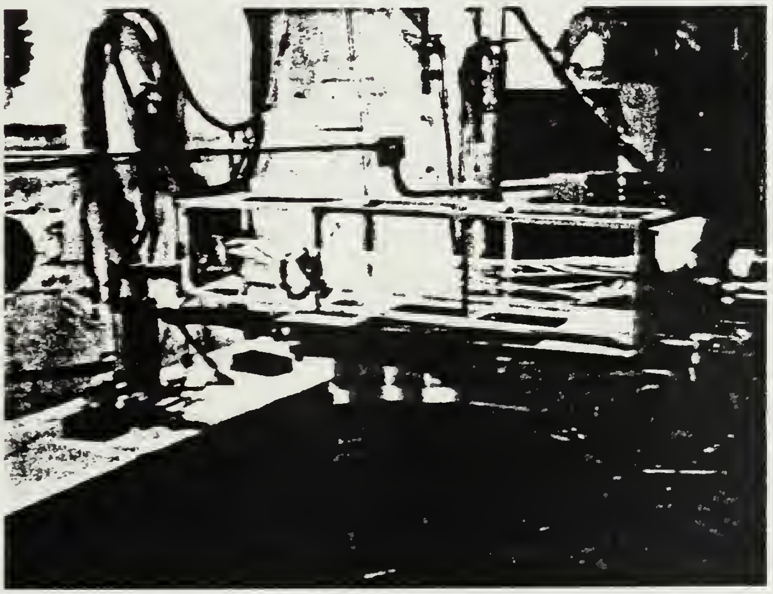

Figure 4. Experimental setup

radiation. The traveling wave tube (TWT) amplifier and a band pass filter of the experiment in Ref. 3 and Ref. 7 are not used. Instead, a crystal detector is attached directly to the end of the waveguide, and then an amplifier is used after that. A Hewlett Packard plotter (HP7090A) is used to record the data. A HP236 computer is used to save and control the data. For normalization of data, a toroid is put on the end of beam pipe to detect the fluctuation of the beam intensity.

It was decided to find the frequency components of the average radiated power in the X-band region (8.2-12.4 GHz) where third harmonic Cerenkov radiation (8.568 GHz for the LINAC) can be detected. For this experiment, the setup is roughly divided into two sections as shown in Figure 5. One is the end station where radiation is detected and transferred to the control room. The other is the control room where data is recorded and saved for further investigation.

1. The end station

The end station is equipped with a toroid, a beam monitor, a aluminum plate, a helium bag, a feedhorn assembly, and two research amplifiers. The electron beam bunches come from the LINAC through the beam pipe which may produce diffraction transition radiation (DTR), and through a plastic KAPTON aperture which may generate transition radiation (TR). On the end of the beam pipe, a toroid is

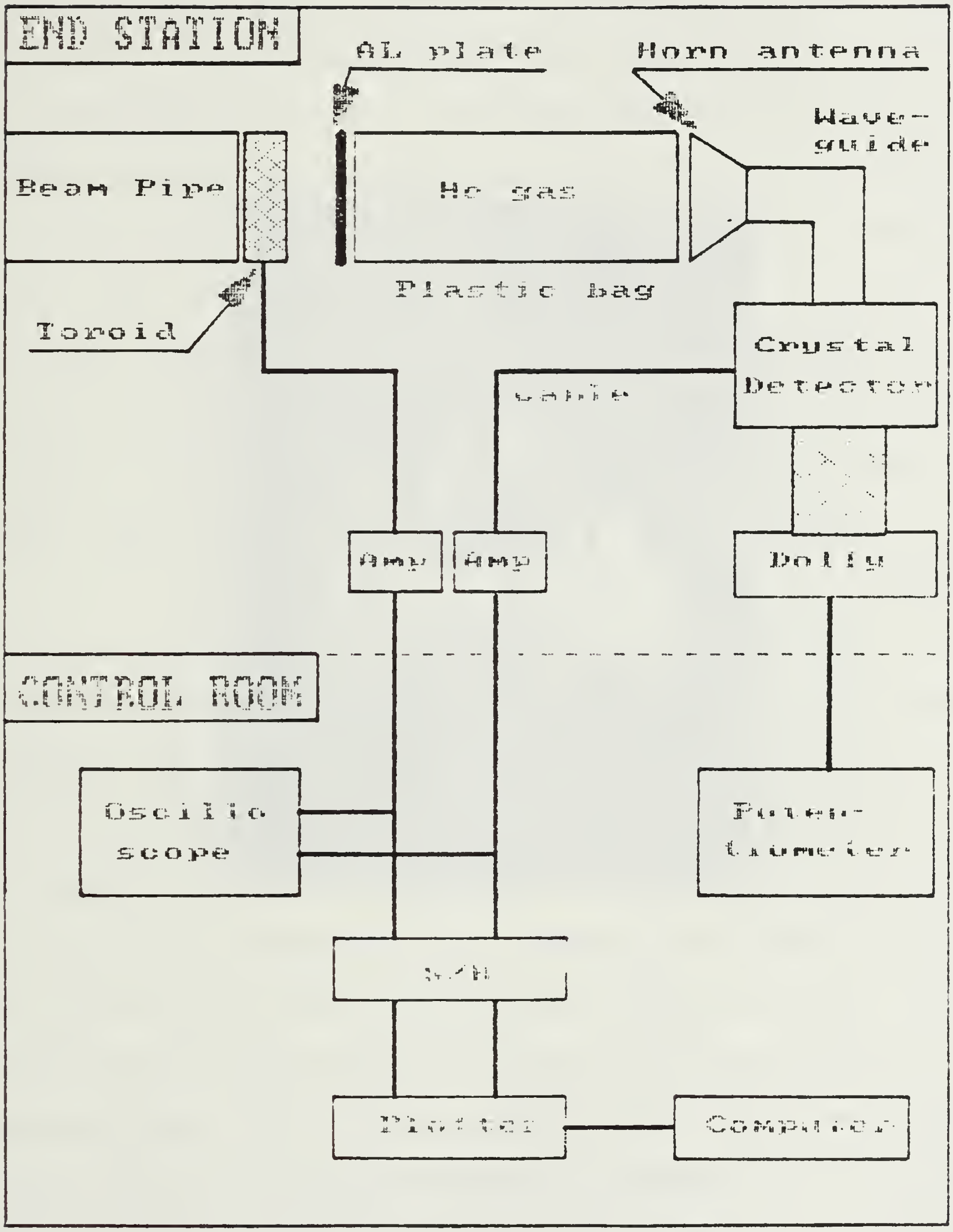

Figure 5. Schematic diagram of the setup

located to detect the fluctuation of the beam intensity. The toroid output is used for normalization of the detected signal from the feedhorn antenna. After the toroid, the beam goes through the short interaction region in air where Cerenkov radiation is generated. A 14 cm interaction region separates the end of the beam pipe and the aluminum plate to provide a far field detection of Cerenkov radiation. A 27 cm X 36 cm X 0.05 cm aluminum plate (without hole) is used for TR and three plates (each with a different hole size) are used to detect DTR. A plastic bag containing helium gas is used to eliminate the Cerenkov radiation which is produced when air is between the plate and the feedhorn assembly.

The feedhorn assembly, Figure 6, consists of a horn antenna, a short piece of waveguide, a crystal detector, a mounting assembly, and a travelling dolly. The X-band 3.1 cm X 4.6 cm microwave horn antenna is located at 1.5 m away from the plate. A 29.5 cm section of X-band waveguide is inserted between the antenna and the crystal detector, which is bent down to protect the detector from the electron beam. The crystal detector is used for modulating the radiation to visible to the oscilloscope and to the sample-and-hold network in the control room. The mounting assembly holds the feedhorn and allows the feedhorn to rotate though the angle to measure the angular dependence of the direct radiation. The center of the horn antenna is located along the axis of

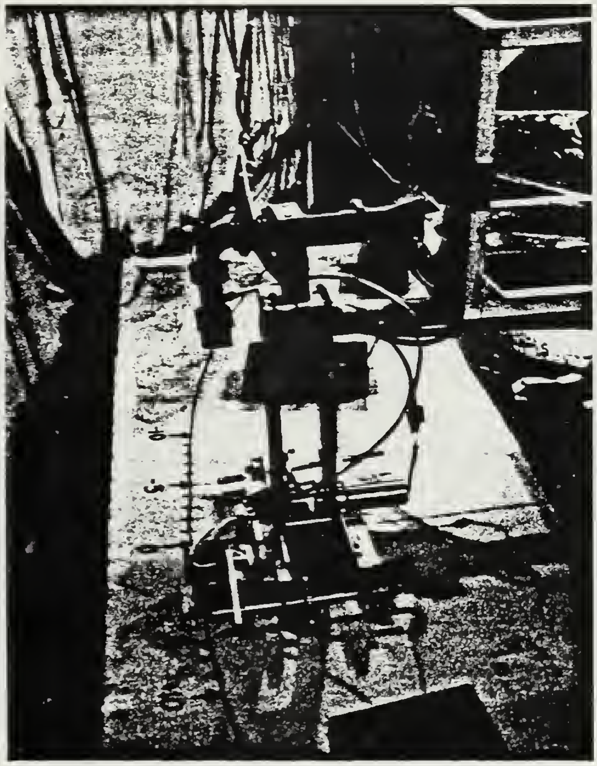

Figure 6. Feedhorn assembly

the beam and maintained at the same vertical level while rotating from side to side by a traveling dolly. The traveling dolly carries the feedhorn assembly and travels along a wooden platform on which the angles are marked. The speed of the traveling dolly is controlled by a potentiometer in the control room. A camera and a monitor is established to see the angles. The microwave signal received at a feedhorn, modulated by the crystal detector, is transmitted to the research amplifier through RG 9/U coaxial cable. A relatively weak signal is amplified with two amplifiers with maximum 3000 gain. One is for the beam signal, the other is for radiation. These amplified signals are transmitted to the control room by triply shielded cable.

2. Control room

Signals from the end station are split and sent in two directions in the control room. One direction leads to an oscilloscope for visual reference, and the other to the data collection network as shown in Figure 7. The data collection network consists of a sample and hold network, an oscilloscope, a plotter, and a computer. The integrated circuit high speed sample-and-hold network is well explained with Figure 17 and 18 in Reference 7. Another oscilloscope is used for integration timing for the sample-and-hold network.

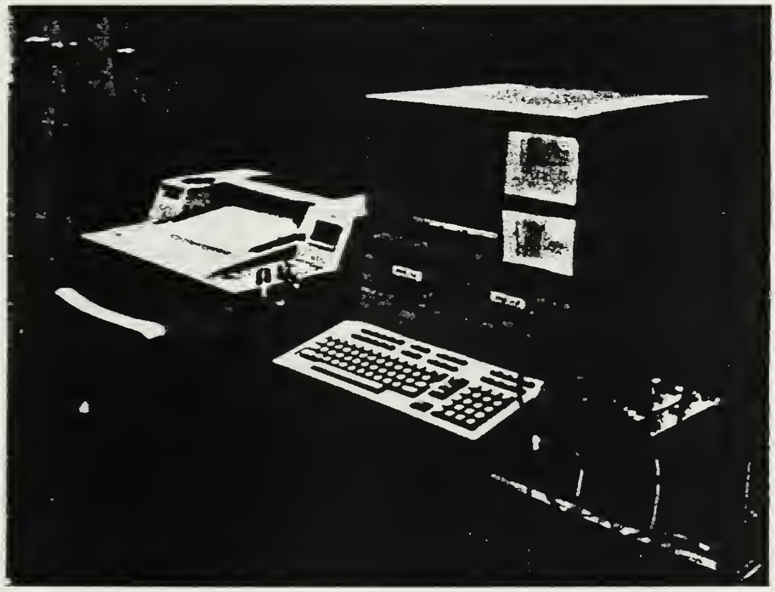

Figure 7. Control room

After this network, signals are transmitted to the programmable HP7090A plotter through two channels, one to observe the beam current and the other to record the radiation signal. The plotter can take one thousand digitized data per each channel during a given period. Then, it can plot the data itself or be controlled by a computer. The HP236 computer was used to control the plotter and save the raw data and provided a program written in Basic language,. Also, it used another program for further investigation (see Appendix 2).

B. PROCEDURE

1. Digitization

This experiment can be divided roughly into three steps. The first step is the digitization of the data. In most experiments at NPS, data was obtained by manually recording values from the oscilloscope or from the spectrum analyzer at angles observed through the closed circuit television. It was significantly improved by Bruce [Ref. 7] using the X/Y recorder in which the data was recorded automatically. However, all data was analog in form and no manipulation of data was possible because of its analog nature.

This problem was solved by using a HP7090A plotter as shown in Figure 8. Three channels are available for receiving analog input signals and each channel uses its own

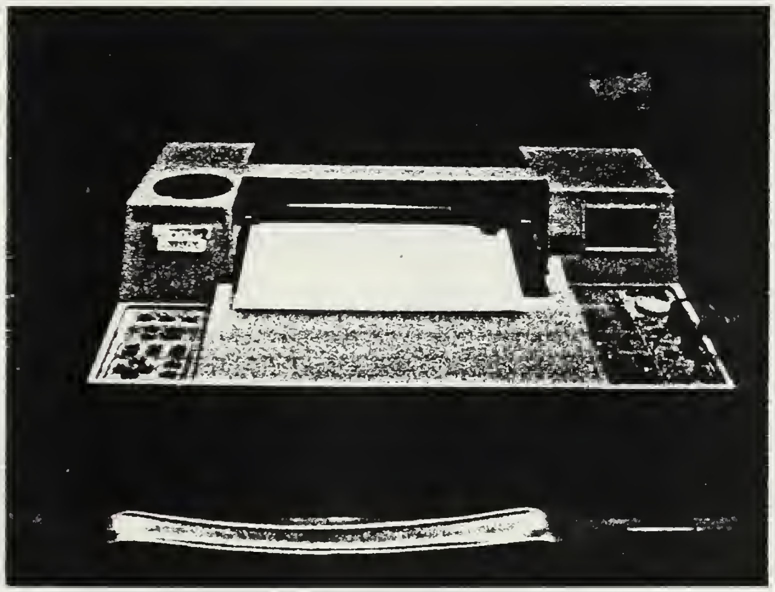

Figure 8. HP7090A plotter

analog-to-digital (A/D) converter to digitize the analog input. It contains three buffers that are used to store digitized input signal data during buffered recording and each buffer is capable of storing 1000 data values in a given period. The period for acquisition of the signal can be set from 1 sec to 24 hours. This buffered data can be used for drawing or for transferring to the computer. Also, It can plot the modified data from a computer. That is, the plotter serves as the front end of a data acquisition system or as a graphics plotter with a computer.

2. Normalization

The next step is normalization of the signal. Since the radiation field is dependent on the beam current, The observed field signal should be corrected when the beam changes. This correction is called normalization. If the beam is constant, the signal should be stable when the detector is fixed. First, two antennas were used at two fixed positions during a 30 second period. Then, Cerenkov radiation detected with both antennas is continuously changed as shown in Figure 9. To normalize, average value of one signal is calculated then it is applied to the other signal to compensate for fluctuations. But it was over corrected as can be seen in Figure 9.

Many methods were tried to accomplish normalization. It was assumed that the relation of the signal and the beam was linear according the equation (8). A toroid was used to

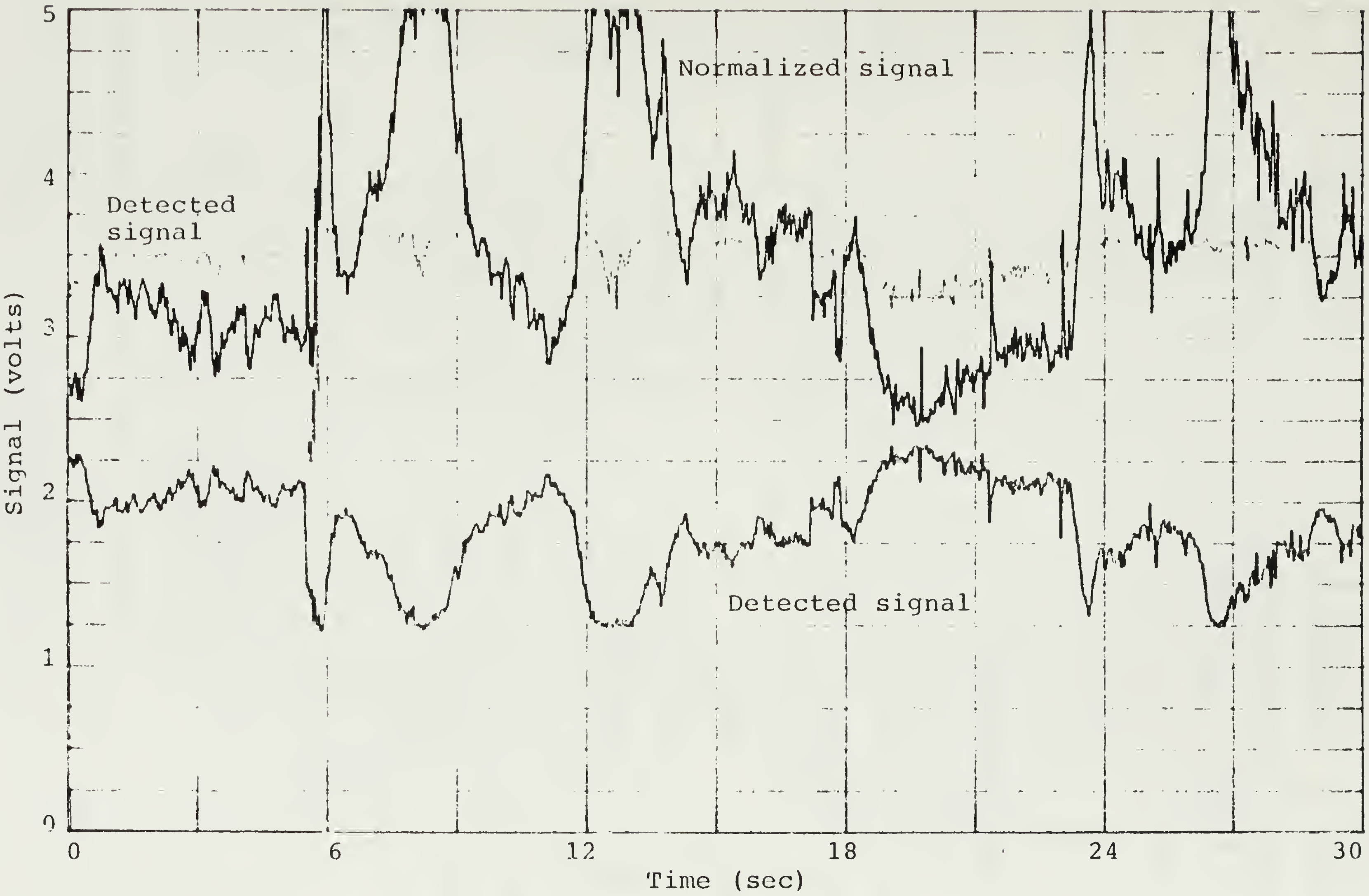

Figure 9. Detected and normalized signal

detect the changes in the beam. Although this is not sufficient for normalization since the relation between the beam current and the radiation signal is not exactly known. Another problem encountered during the programming for normalization. Since the beam current occasionally goes to zero, previous value is assumed for the value of zero (see Appendix 2).

3. Data collection

The collecting data is the third step of this experiment. During the data acquisition, it was noticed that the alignment of the antenna is very important. The height of both lobes is very dependent on the positioning of the antenna. When the antenna is aimed to the right relative to an observer facing in the beam direction, the left lobe is higher than the right lobe as shown in Figure 10. In the other case, aiming to the left, the right lobe is higher than the left lobe (Figure 11). So alignment of the antenna is carefully checked to see if the axis of the antenna is the same as the axis line of the beam.

The intensity of the detected signal from the antenna is affected by beam focusing. The beam is blurred when the focal point is moved further from the end of the beam pipe, due to the diffusion of the beam in air. Consequently, it is difficult to focus at a point downstream from the beam pipe (see Figures 12, 13, and 14). When the distance of the antenna from the beam pipe is fixed to

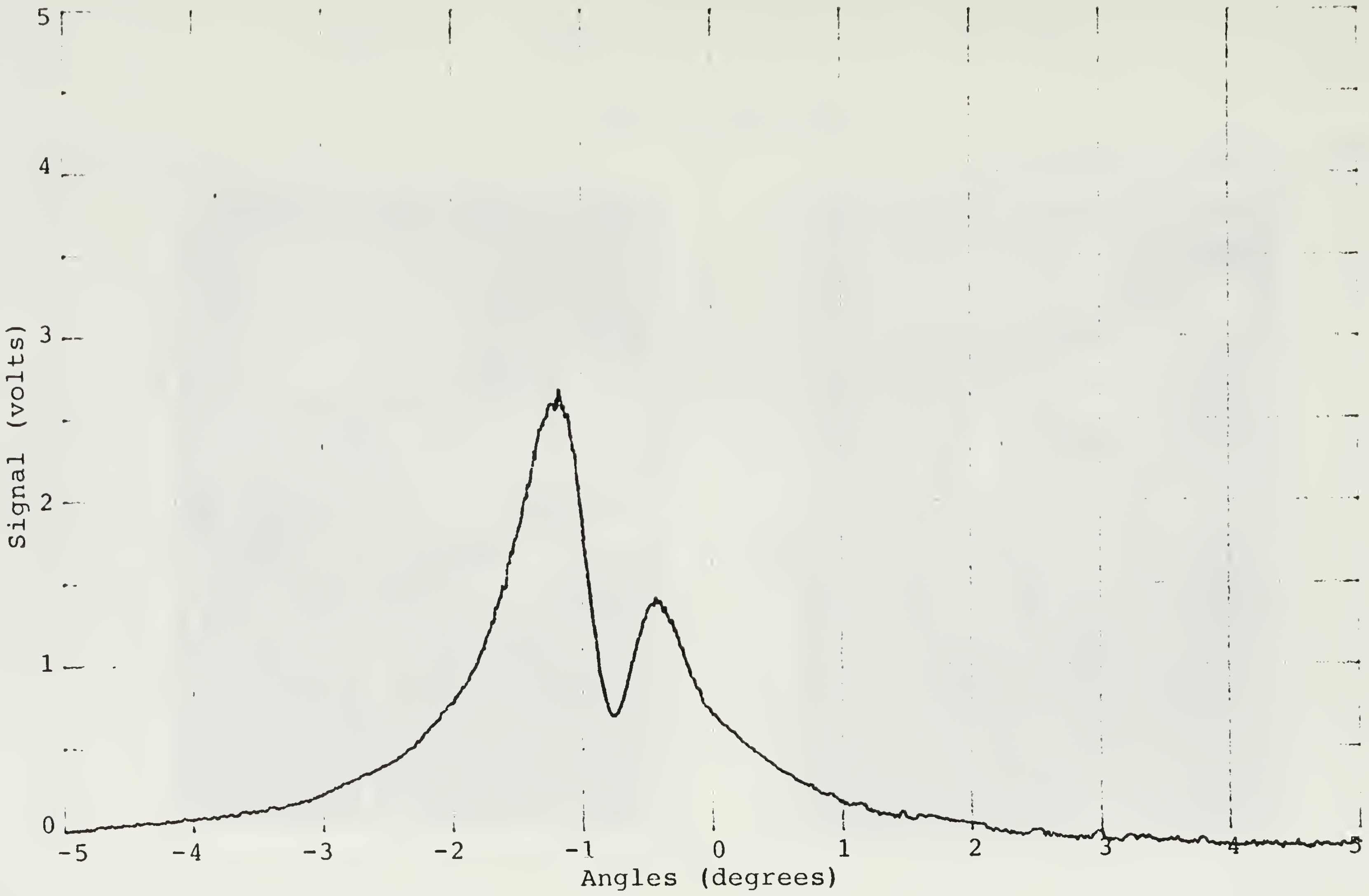

Figure 10. Signal by tilting to the 15° right

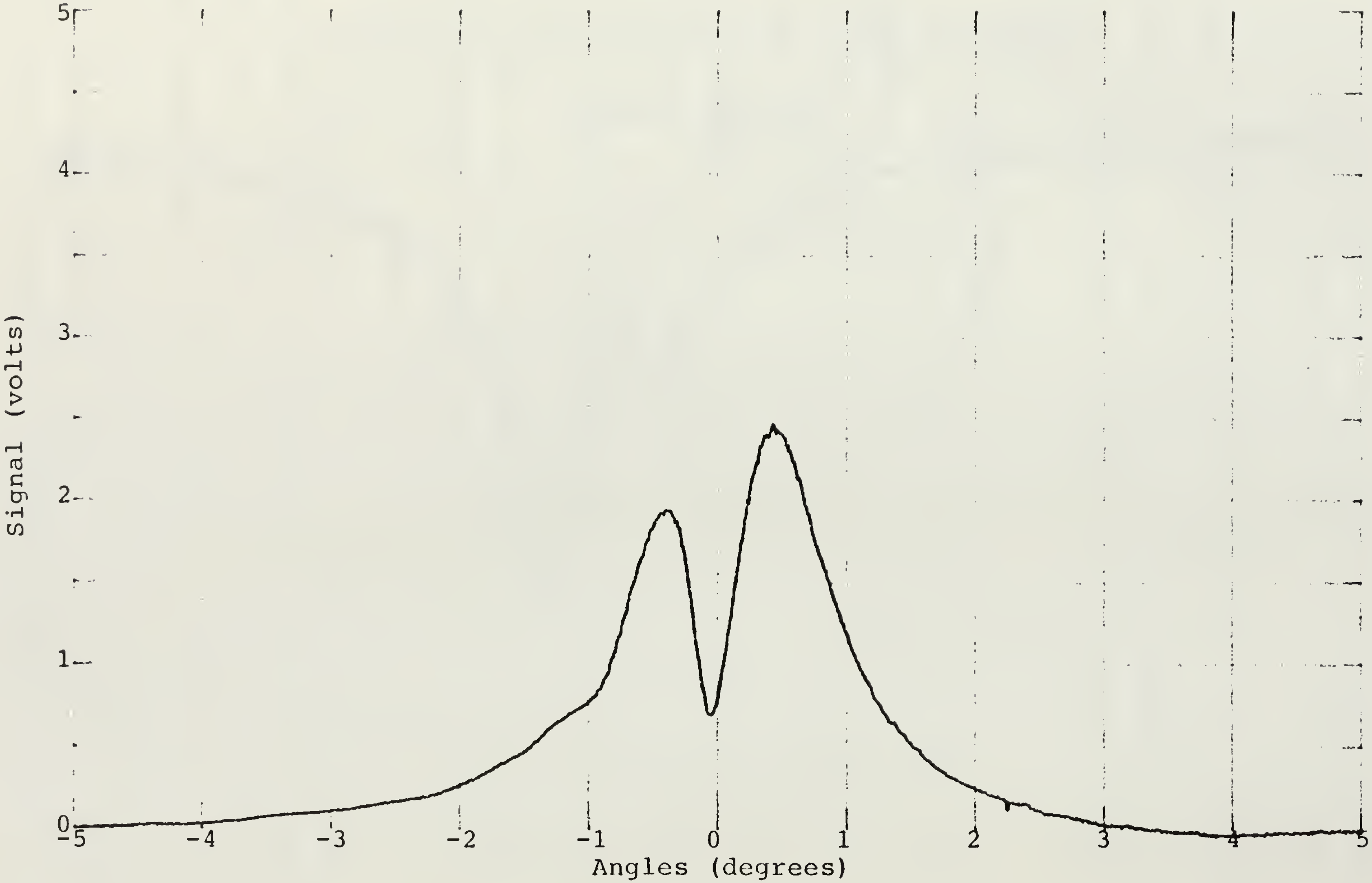

Figure 11. Signal by tilting to the 15° left

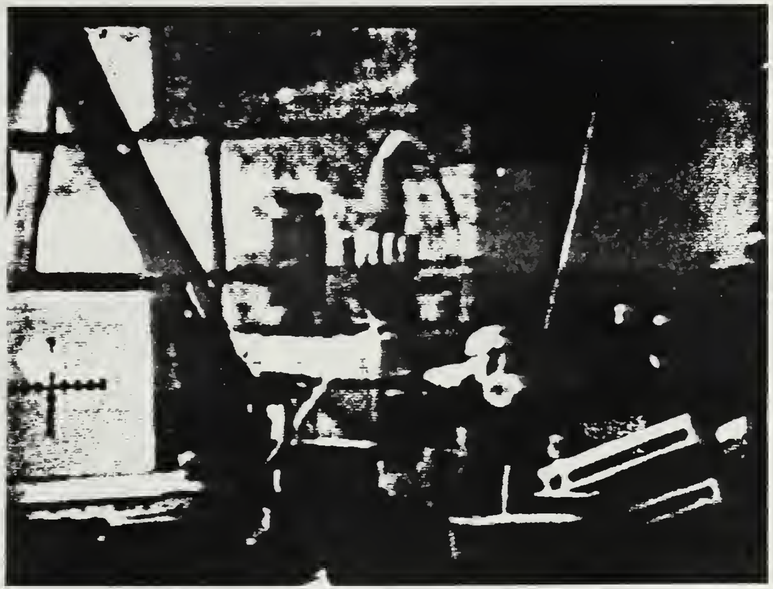

80 cm

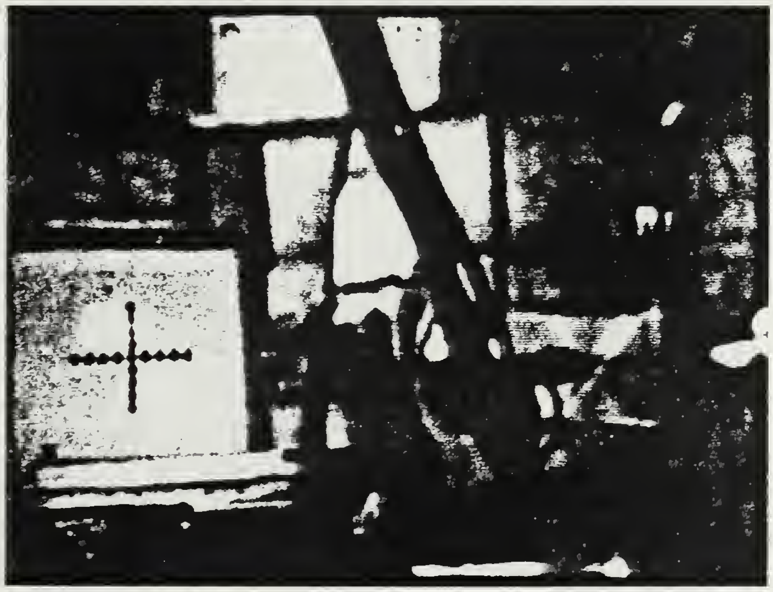

100 cm

Figure 14. Beam focusing with distance 80 cm and 100 cm

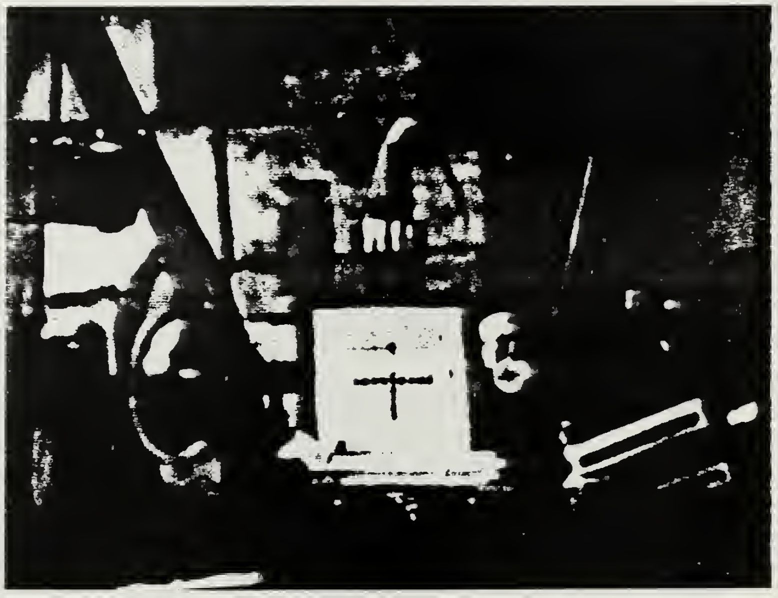

40 cms

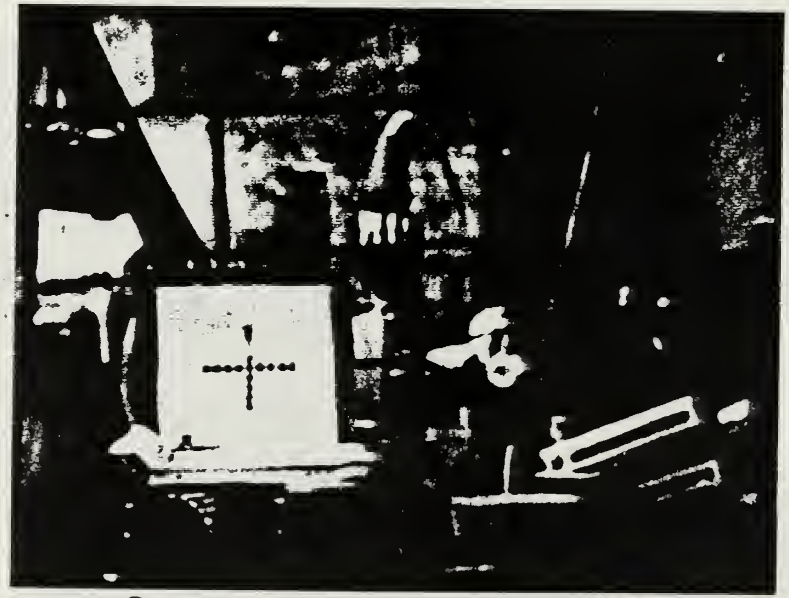

60 cm

Figure 13. Beam focusing with distance 40 cm and 60 cm

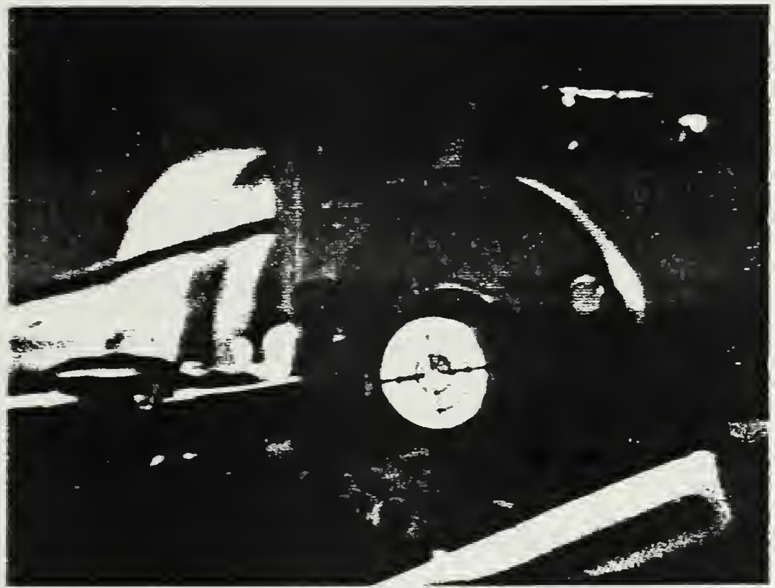

BEST FOCUS, EXIT WINDOW

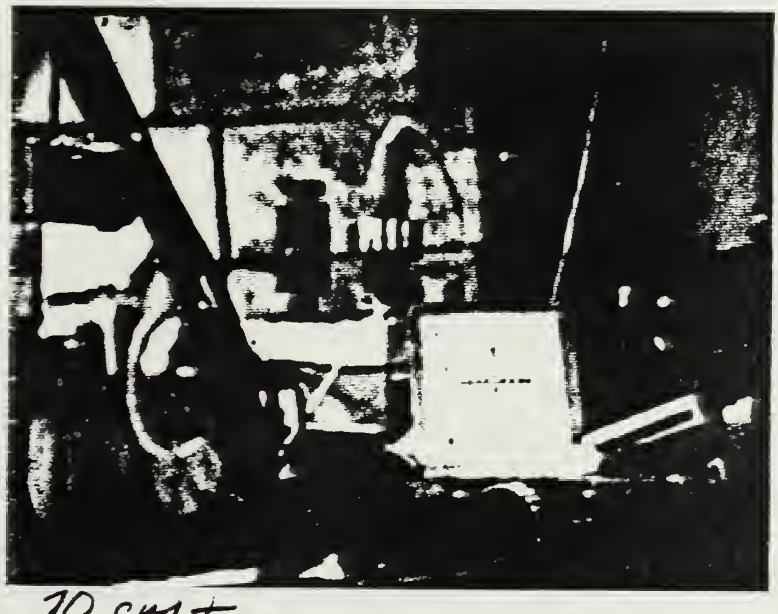

20 cm+

Figure 12. Beam focusing with distance 0 cm and 20 cm

160 cm, the intensity of the signal is highest when the electron beam is focused at a point 15 cm from the beam pipe.

Since TR and DTR are naturally produced from the end of the beam pipe, and Cerenkov radiation is generated in air, several different setups were required to isolate the DTR from TR and Cerenkov radiation as shown in Figure 15. In the setup A, a aluminum plate with a hole which generates DTR is located at 14 cm from the end of the beam pipe, and a plastic bag filled with helium gas was used to eliminate Cerenkov radiation. Three different sizes of hole (radii of 3 cm, 5 cm, and 7 cm) were used to find the effect of the hole size. A aluminum plate without hole, i.e., radius zero cm, is used in the setup B, which generates TR. To remove Cerenkov radiation production in air from the plate to the antenna, helium gas in a plastic bag was used. But the plastic bag itself was a source of another TR and reflection from the plastic bag also must be considered. To find these effects, several setups were used. Setup C uses a helium bag only. Setup D uses the same bag but air instead helium. Setup E uses the same bag without ends. And setup F uses no material (air only) between beam pipe and antenna.

Since all three radiations are produced by a beam bunch moving at a constant velocity and the boundary (KAPTON, aluminum plate, plastic bag ends) is perpendicular to the electron beam, the electric field of all three

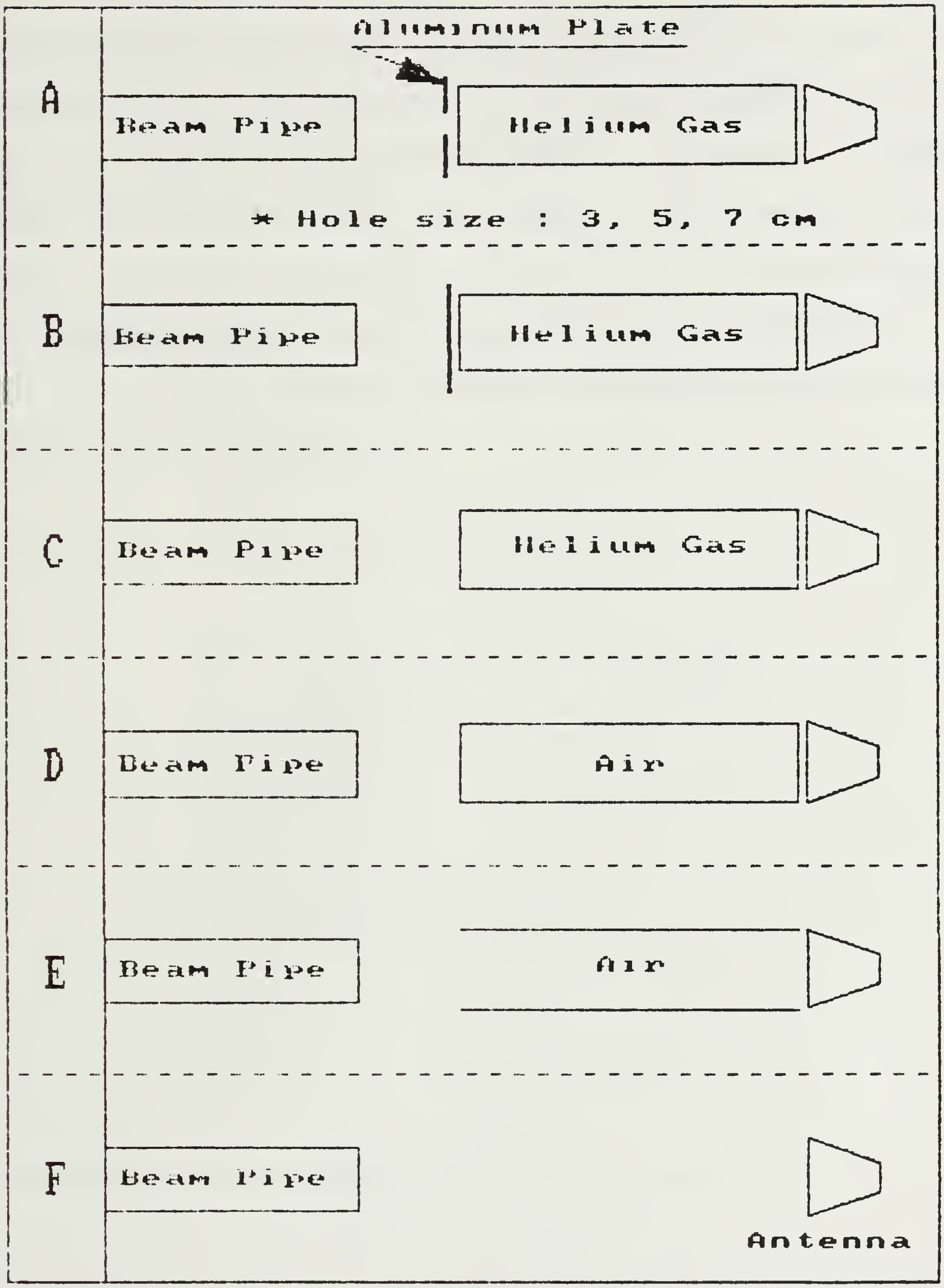

Figure 15. 6 patterns of setup

radiations will be in the plane of the beam direction and the detector. The magnetic field will be perpendicular to this plane. Therefore, it is expected that all three radiations appear together. Although there are no finite boundaries between Cerenkov, TR and DTR, this experiment attempts an empirical separation of the DTR through changes in the setup.

The expected radiations are shown in the Table 1. according to the different setup in Figure 13.

TABLE 1.

EXPECTED RADIATIONS

Setup	Radiations
A	C_{14} + DTR + TR_b + R
B	TR + TR_b + R
C	C_{14} + TR_b + R
D	C_{14} + C + TR_b + R
E	C_{14} + C + R
F	C_{14} + C

In the setup A, it was assumed that the detected signal was consists of Cerenkov radiation from a 14 cm interaction region which is represented as C_{14}. DTR from the aluminum plate with a hole, transition radiation from both ends of a plastic bag which is expressed as TR_b, and some amount of reflection from the side wall of the plastic bag (R). In the setup B, the aluminum plate without hole was replaced and C_{14} in the setup A was removed by this plate. Setup C was same as the setup A except without plate. Setup D used air instead of helium gas in the setup C and therefore Cerenkov radiation was produced inside the bag which is represented as C. Setup E removed the both ends of the plastic bag and setup F removed all material between the beam pipe and the antenna.

III. RESULTS AND CONCLUSIONS

A. RESULTS

Two different energies (32.9 MeV and 63.3 MeV) were used to confirm the experiment. Unfortunately, higher energy was not used because klystron #3 was not operable due to a failure in its associated power supply. Using 32.9 MeV energy, the normalized signal patterns are shown in Figures 16-23 and for 63.3 MeV are shown in Figures 24-31. In reading Figures 16-31, it should be noted that the zero angle could have as much as 1 degree error because the control of the potentiometer and the record starting of the plotter was manually controlled. Measurement of angles covered from -5^0 to $+5^0$. It is also noted that Y-axis is measured as a relative ratio, and the maximum ratio of the detected signal to the beam current was 400 % (except Figures 16, 17, and 21). This scale of X and Y-axis was maintained through the experiments.

The most remarkable aspect of this experiment is that TR and DTR peak angle is closer to the zero angle rather than the peak angle of Cerenkov radiation. In the case of 32.9 MeV, the theoretical peak angle of TR and DTR (0.89^0) is smaller than the theoretical peak angle of Cerenkov radiation (0.98^0). However, the experimental peak angle is

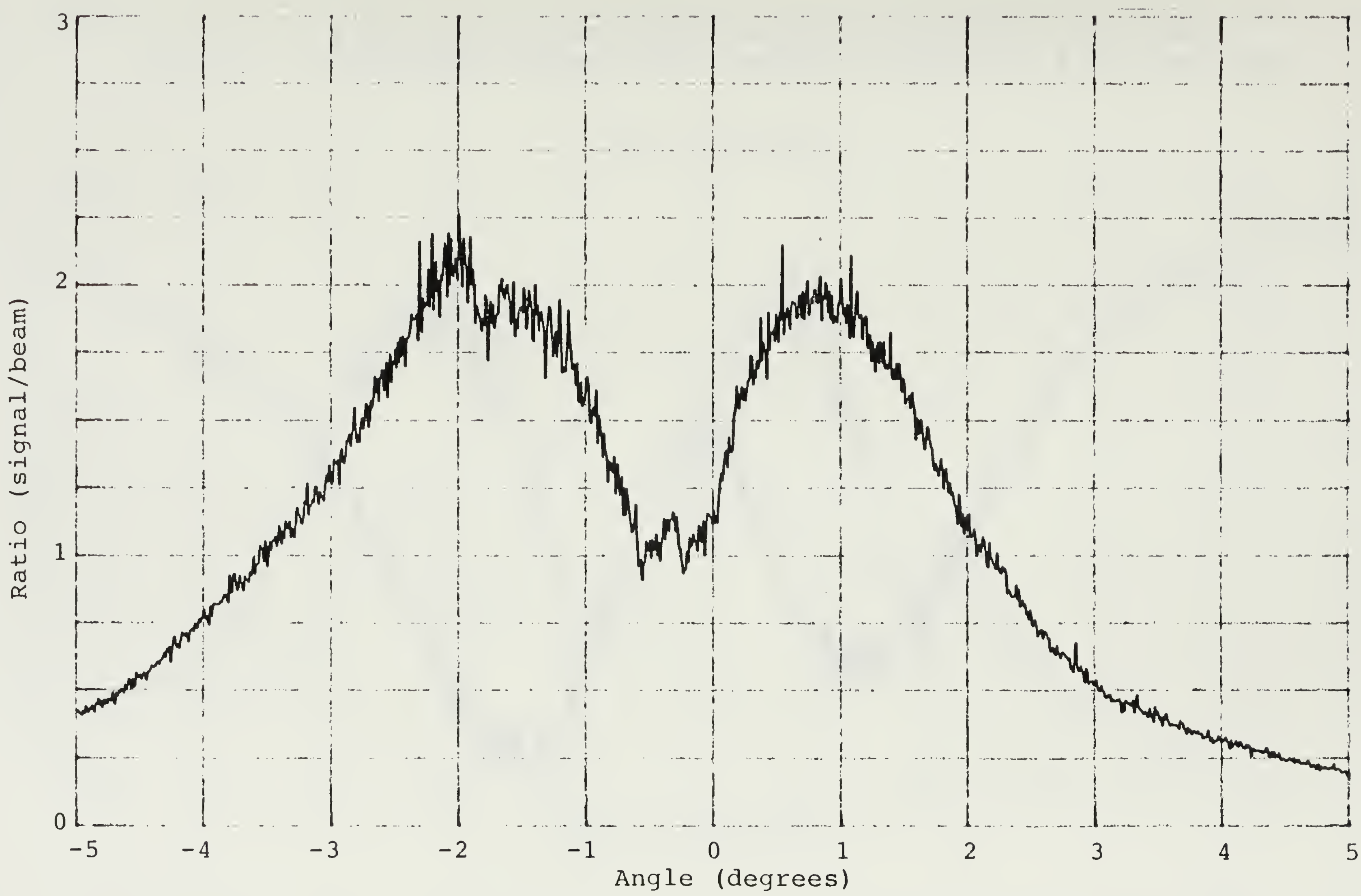

Figure 16. Normalized signal with a radius 7 cm hole in a Al plate and a helium bag (Setup A, 32.9 MeV).

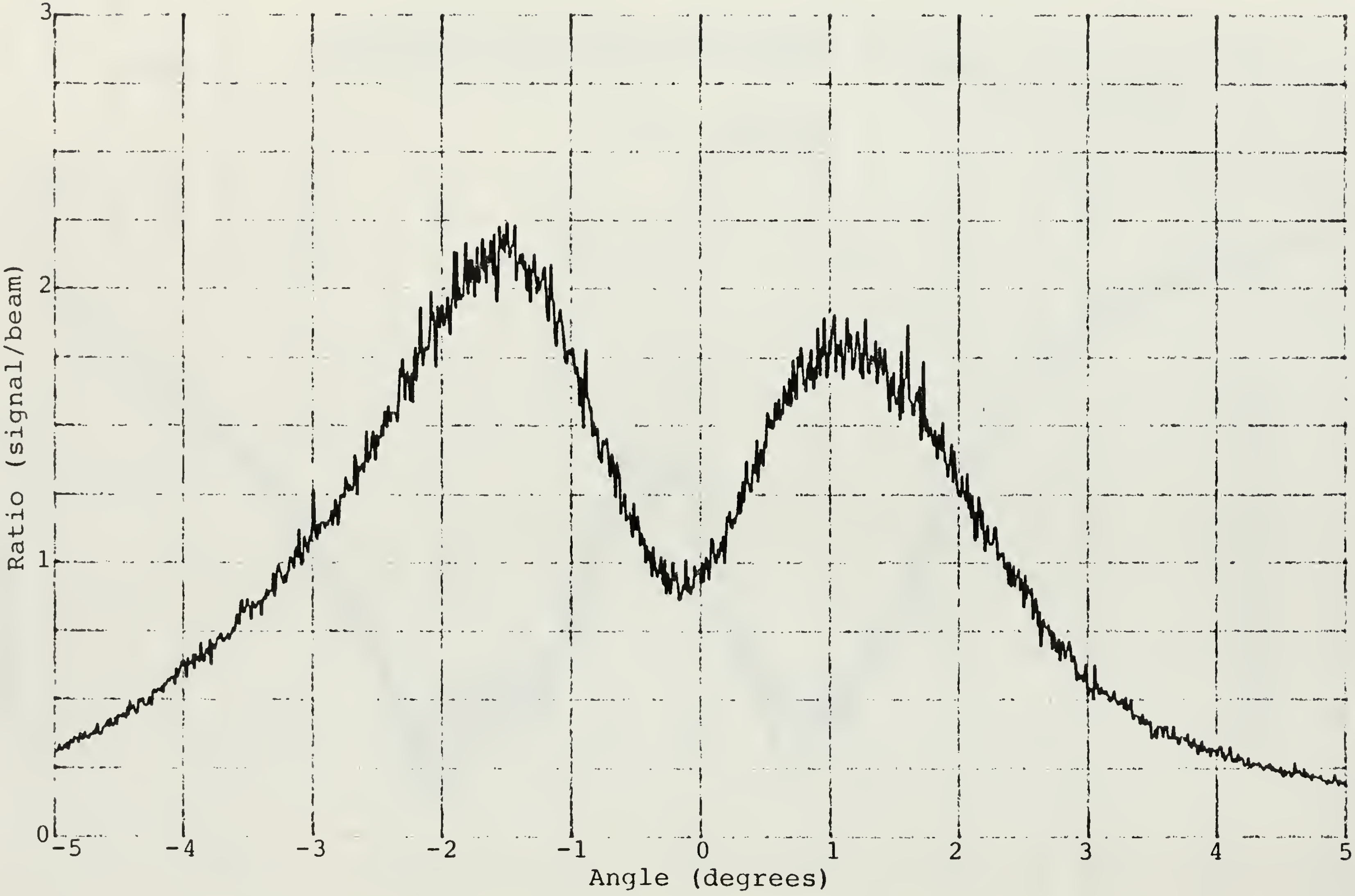

Figure 17. Normalized signal with a radius 5 cm hole in a Al plate and a plastic bag containing helium gas (Setup A, 32.9 MeV).

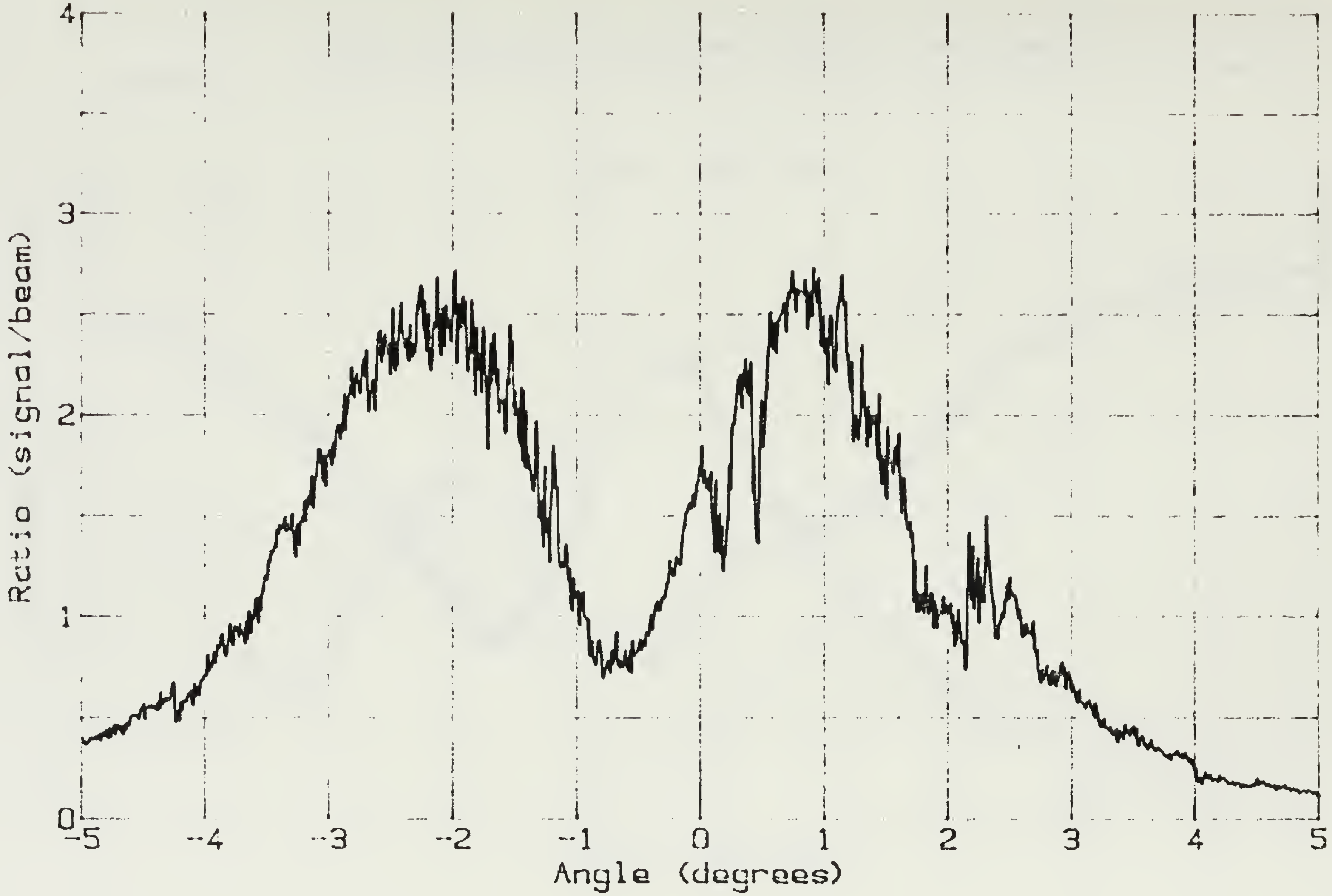

Figure 18. Normalized signal with a radius 3 cm hole in a Al plate and a plastic bag containing helium gas (Setup A, 32.9 MeV).

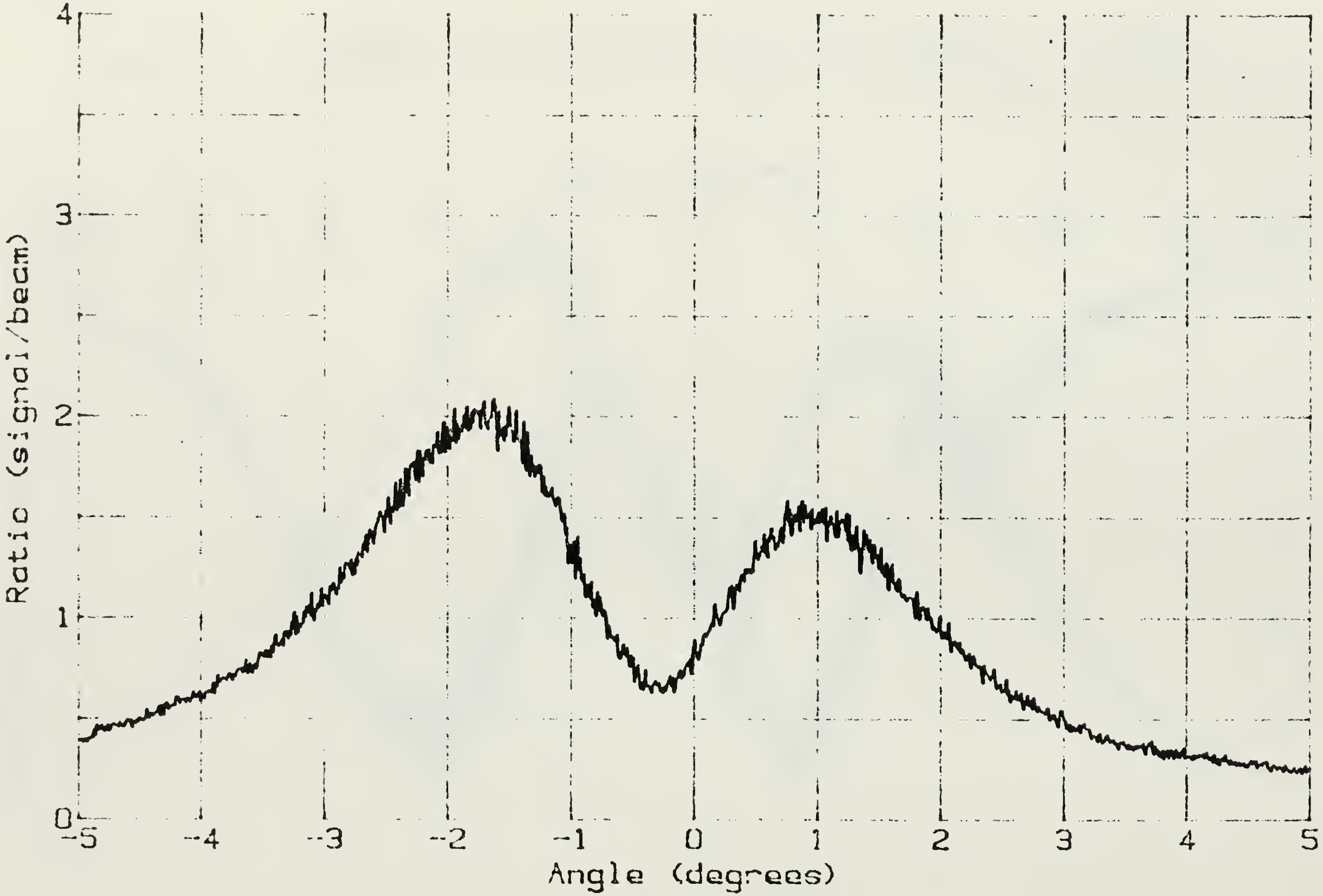

Figure 19. Normalized signal with no hole in a Al plate and a plastic bag containing helium gas (Setup B, 32.9 MeV).

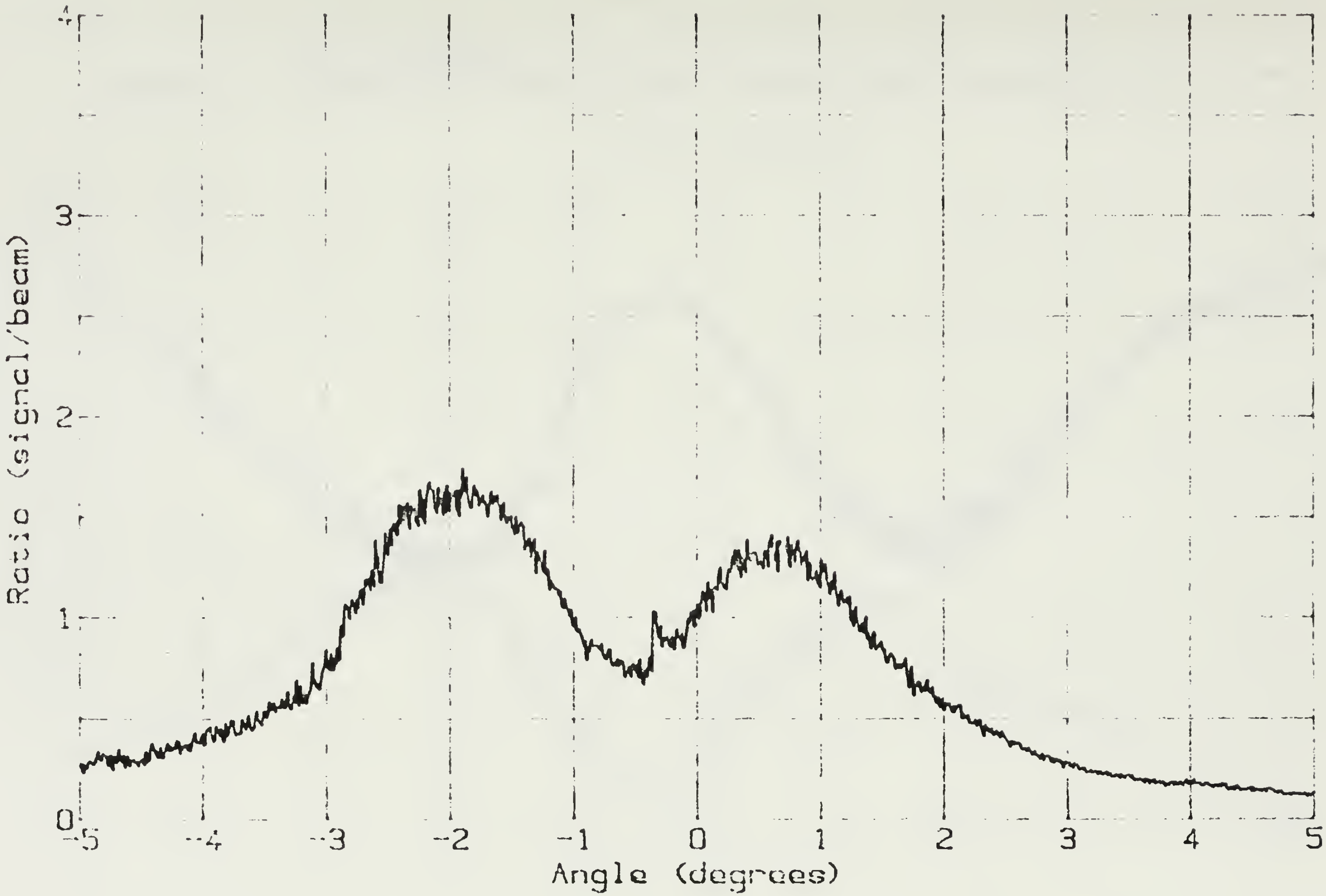

Figure 20. Normalized signal with a plastic bag containing helium gas (Setup C, 32.9 MeV).

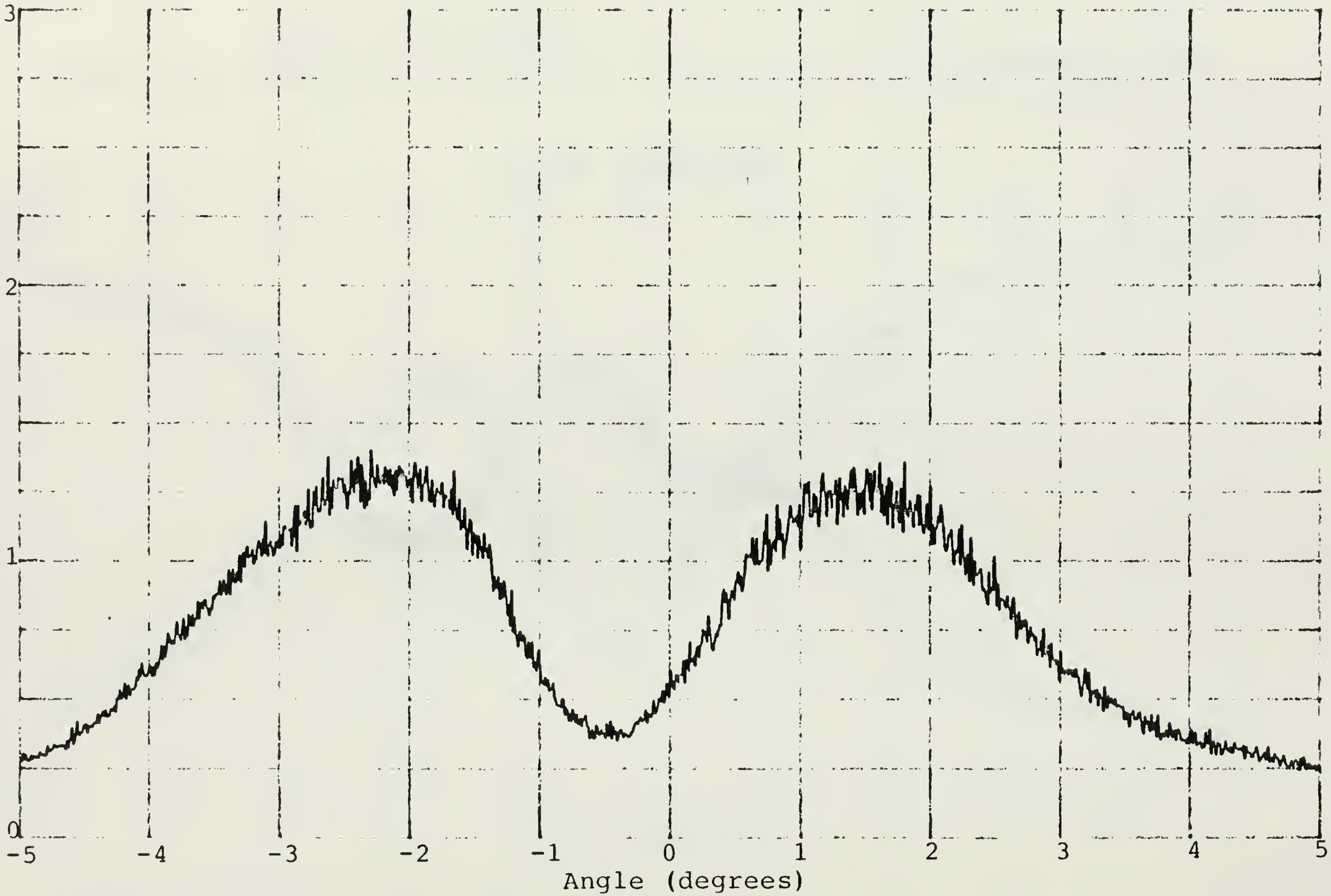

Figure 21. Normalized signal with a plastic bag containing air (Setup D, 32.9 MeV).

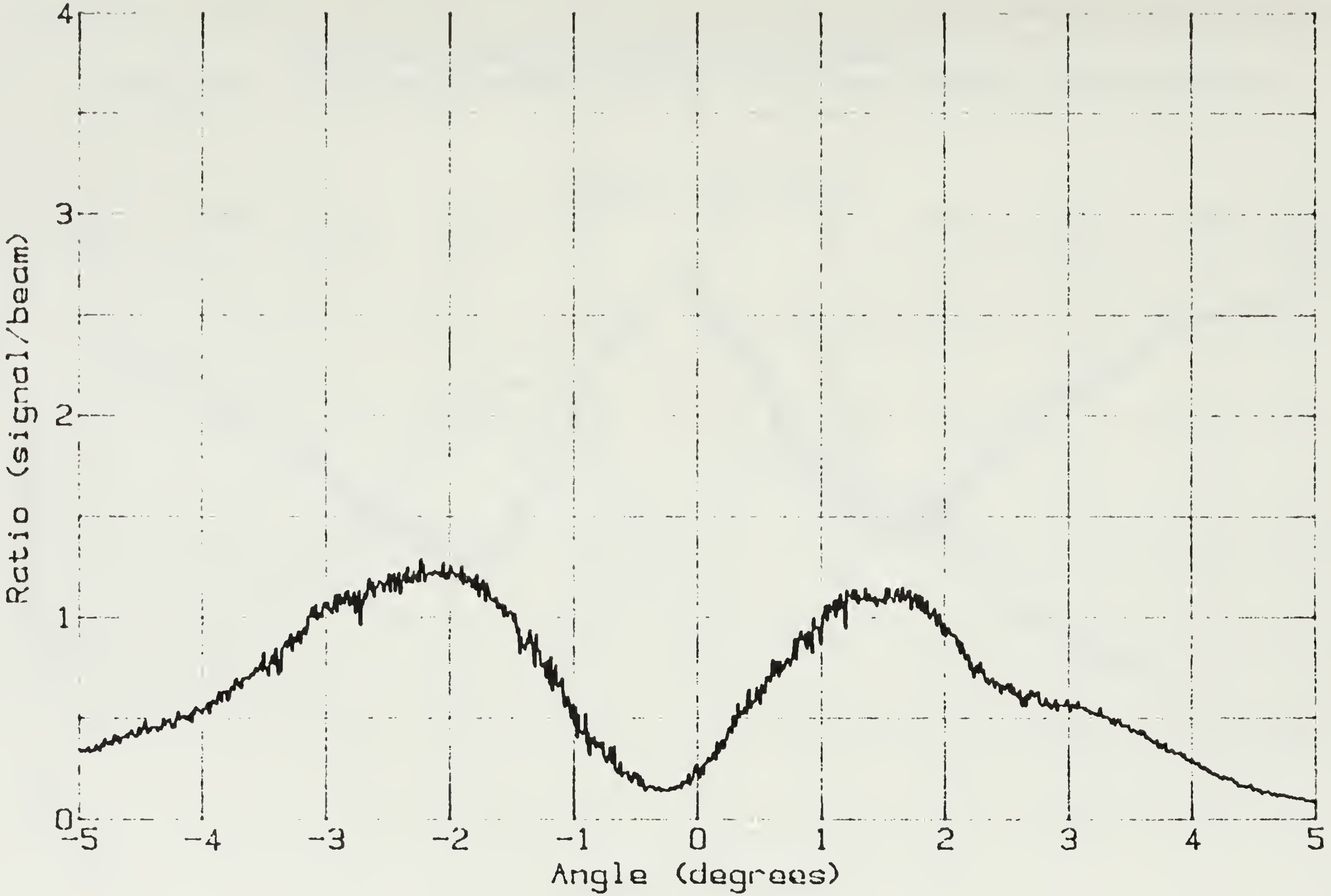

Figure 22. Normalized signal with a plastic tube without ends (Setup E, 32.9 MeV).

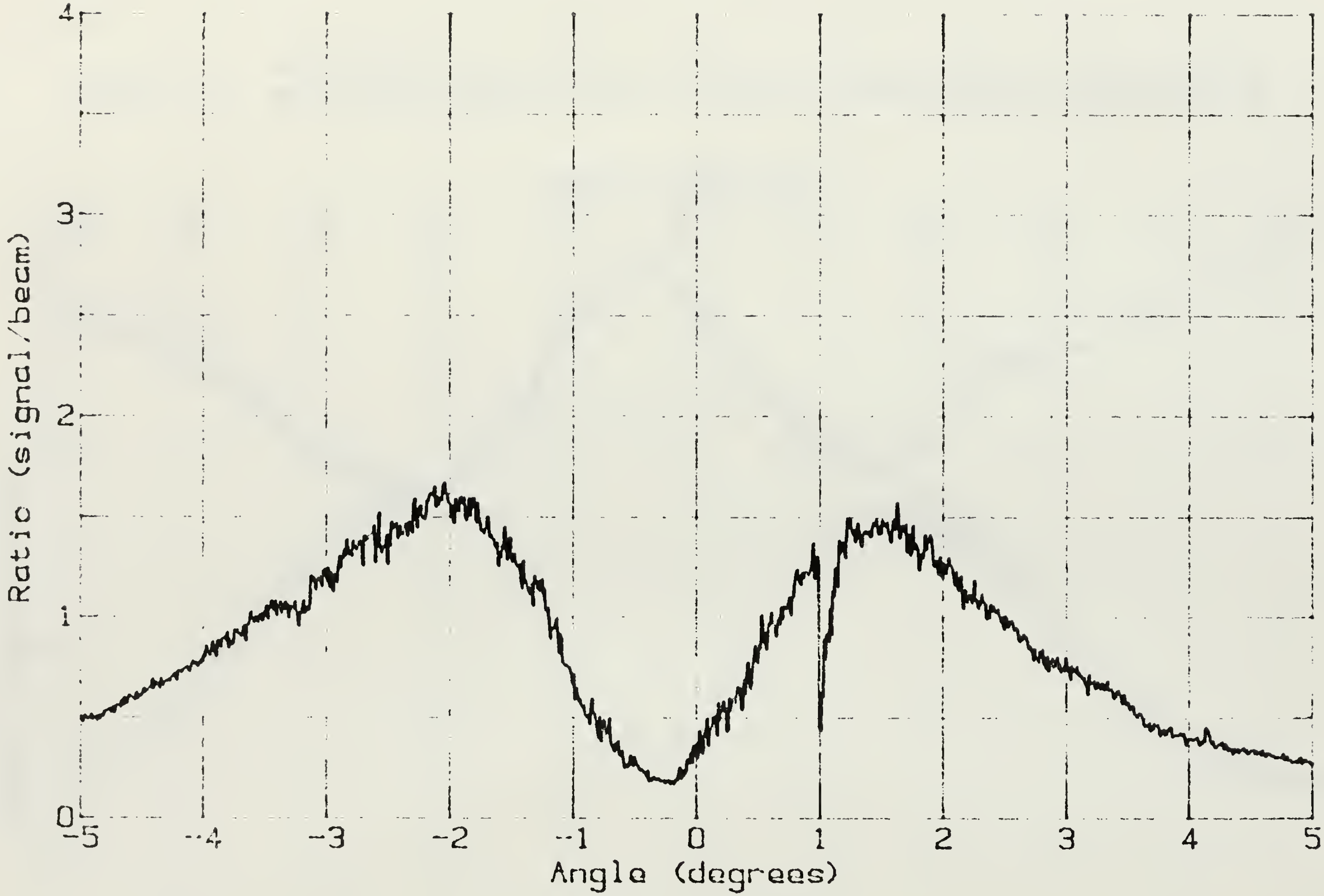

Figure 23. Normalized signal with no materials between the beam pipe and the detector (Setup F, 32.9 MeV).

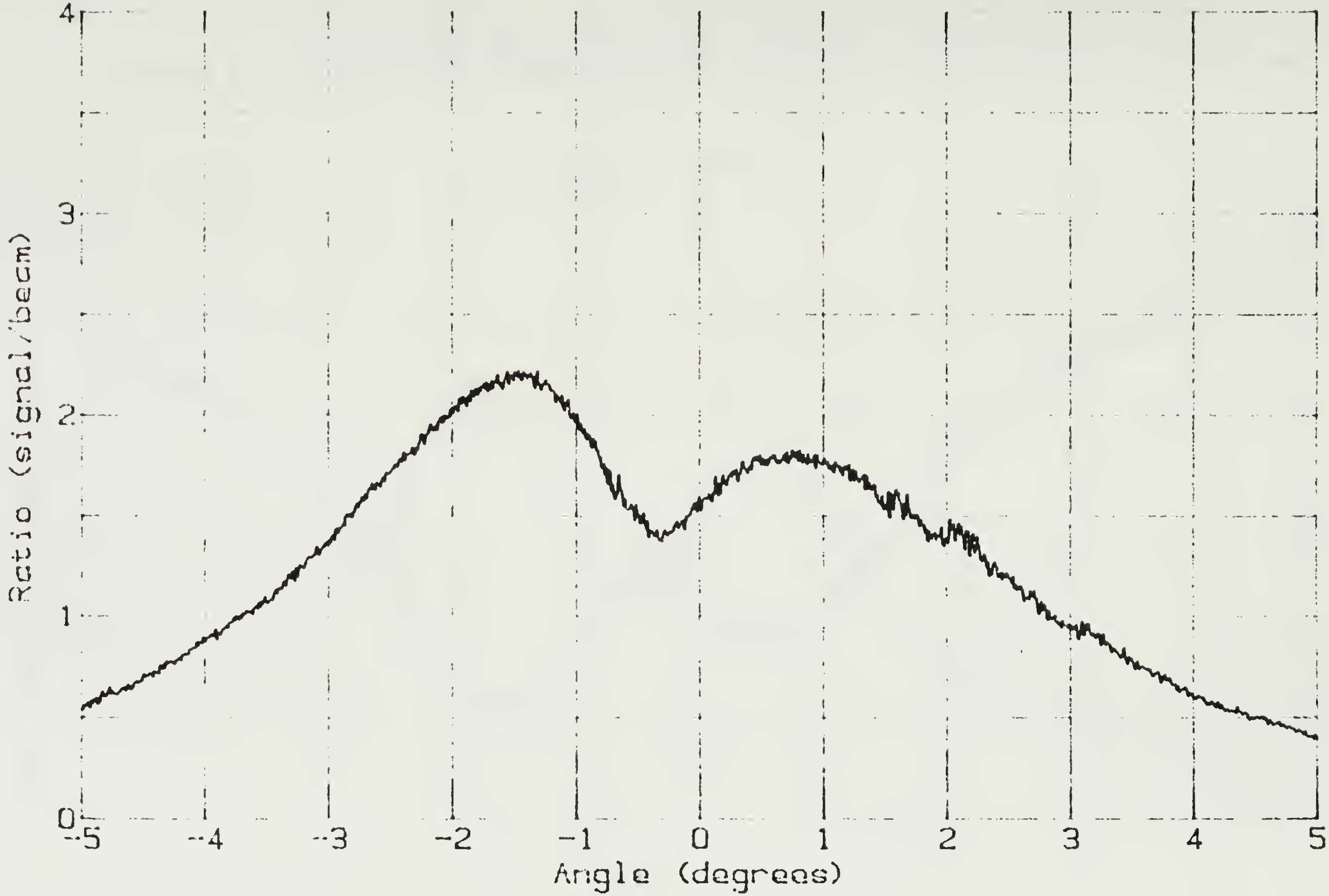

Figure 24. Normalized signal with a radius 7 cm hole in a Al plate and a helium bag (Setup A, 63.3 MeV).

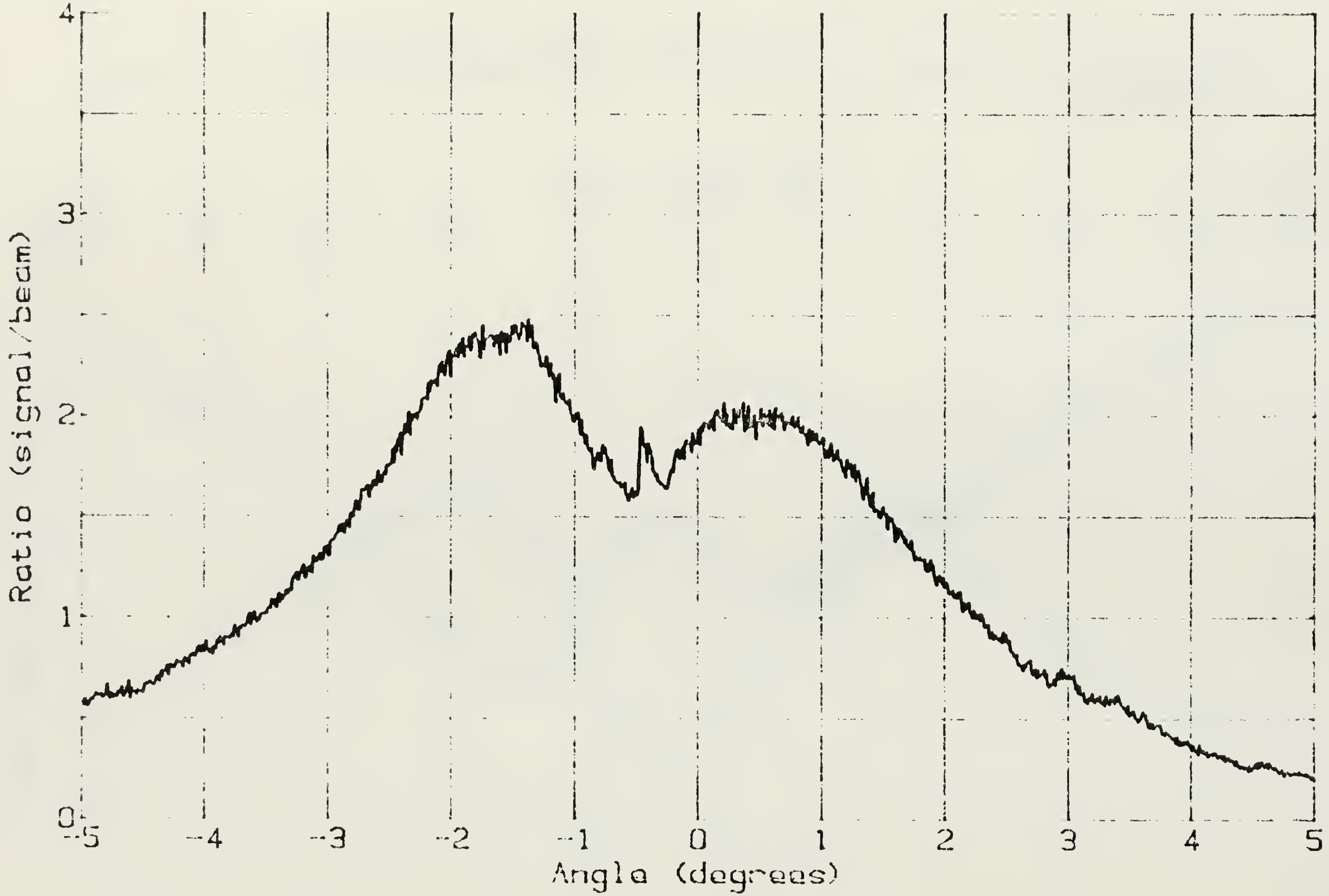

Figure 25. Normalized signal with a radius 5 cm hole in a Al plate and a plastic bag containing helium gas (Setup A, 63.3 MeV).

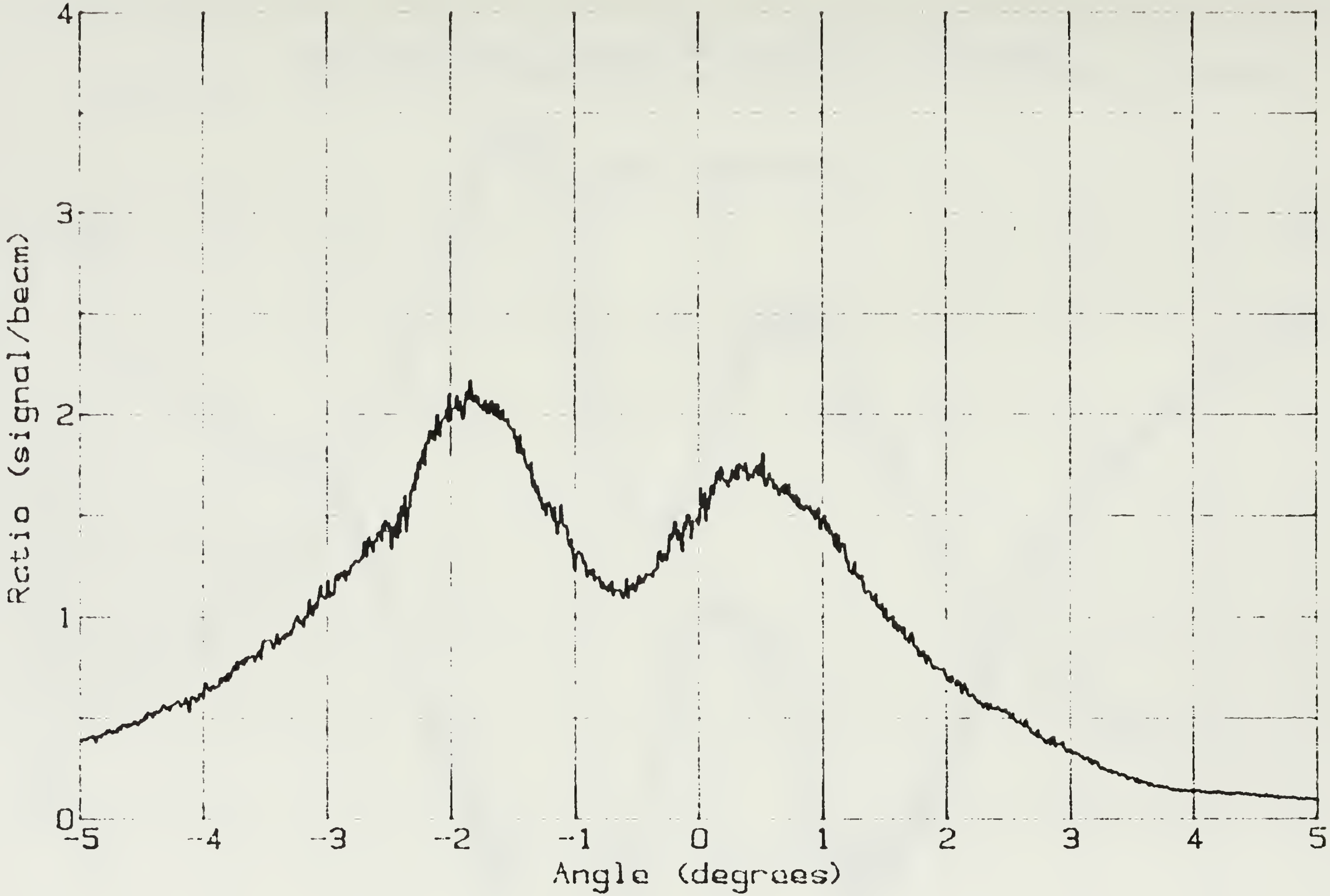

Figure 26. Normalized signal with a radius 3 cm hole in a Al plate and a plastic bag containing helium gas (Setup A, 63.3 MeV).

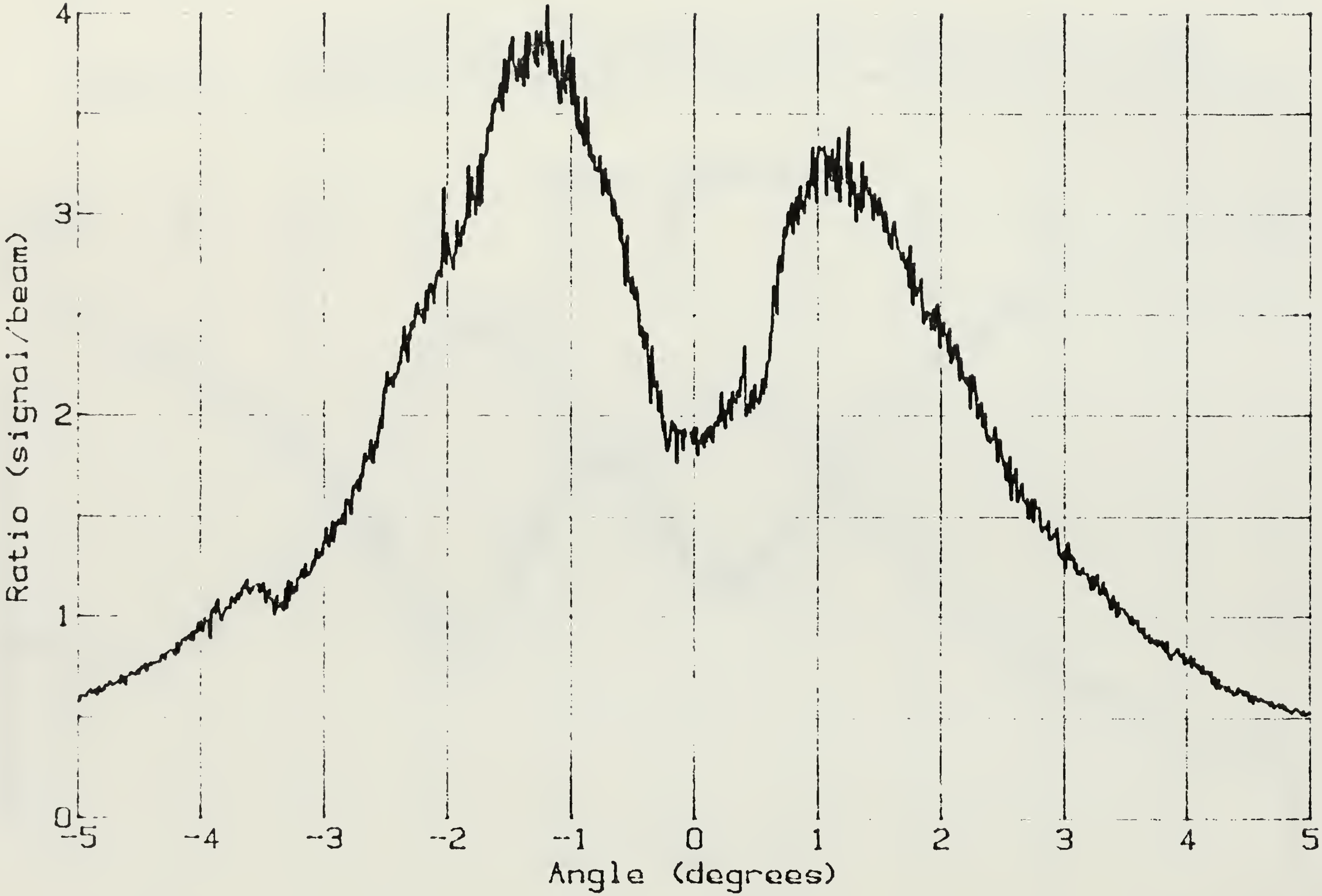

Figure 27. Normalized signal with no hole in a Al plate and a plastic bag containing helium gas (Setup B, 63.3 MeV).

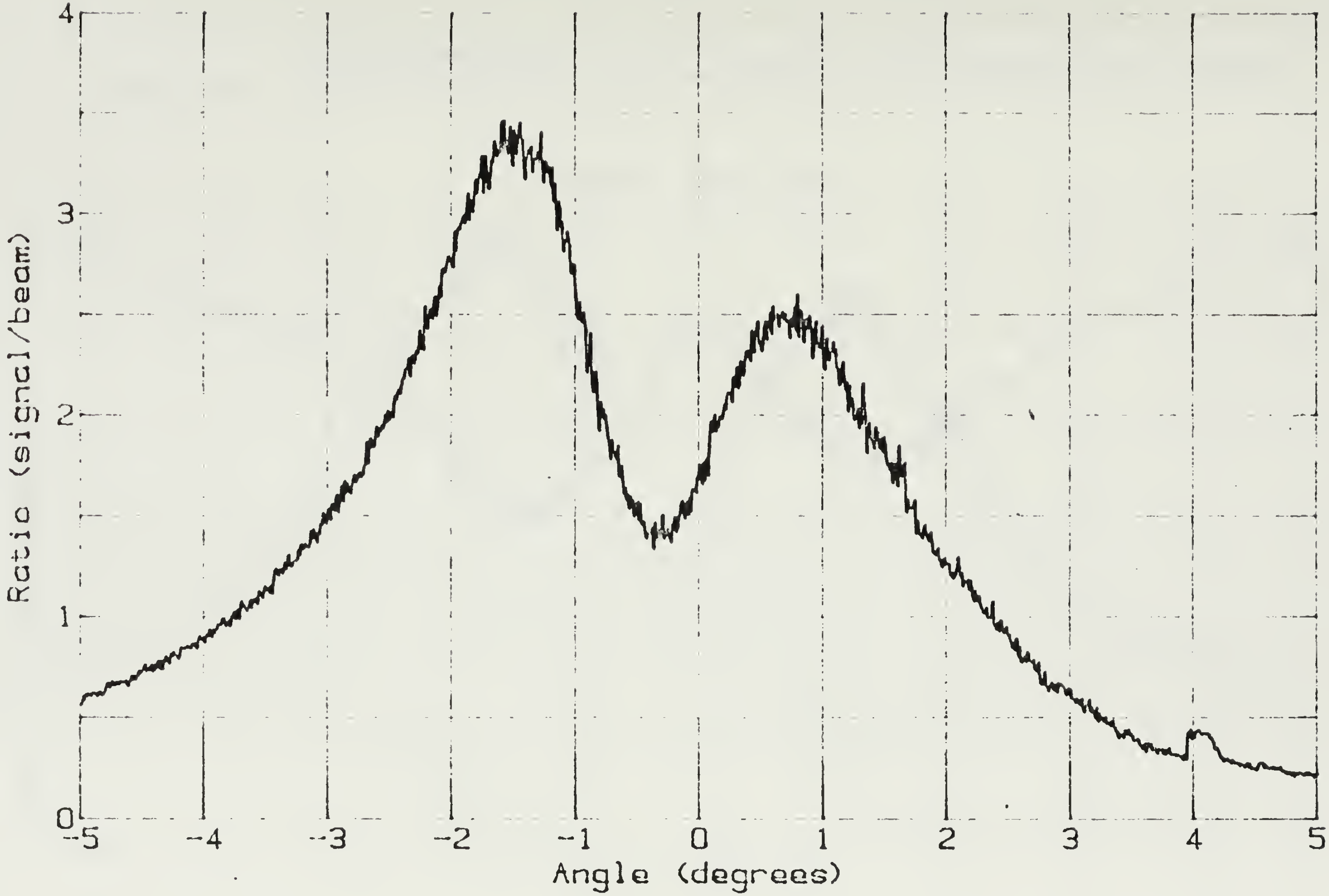

Figure 28. Normalized signal with a plastic bag containing helium gas (Setup C, 63.3 MeV).

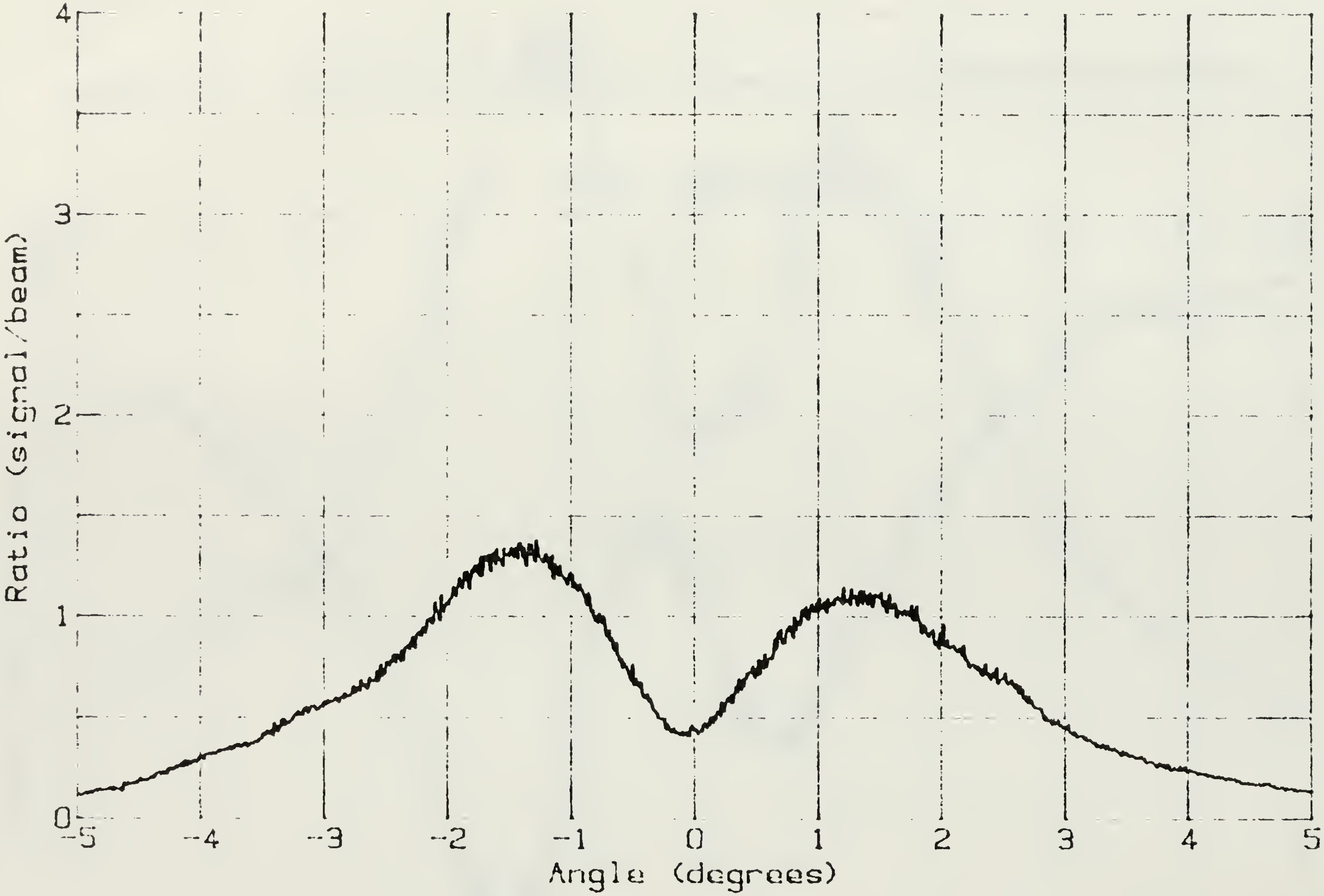

Figure 29. Normalized signal with a plastic bag containing air (Setup D, 63.3 MeV).

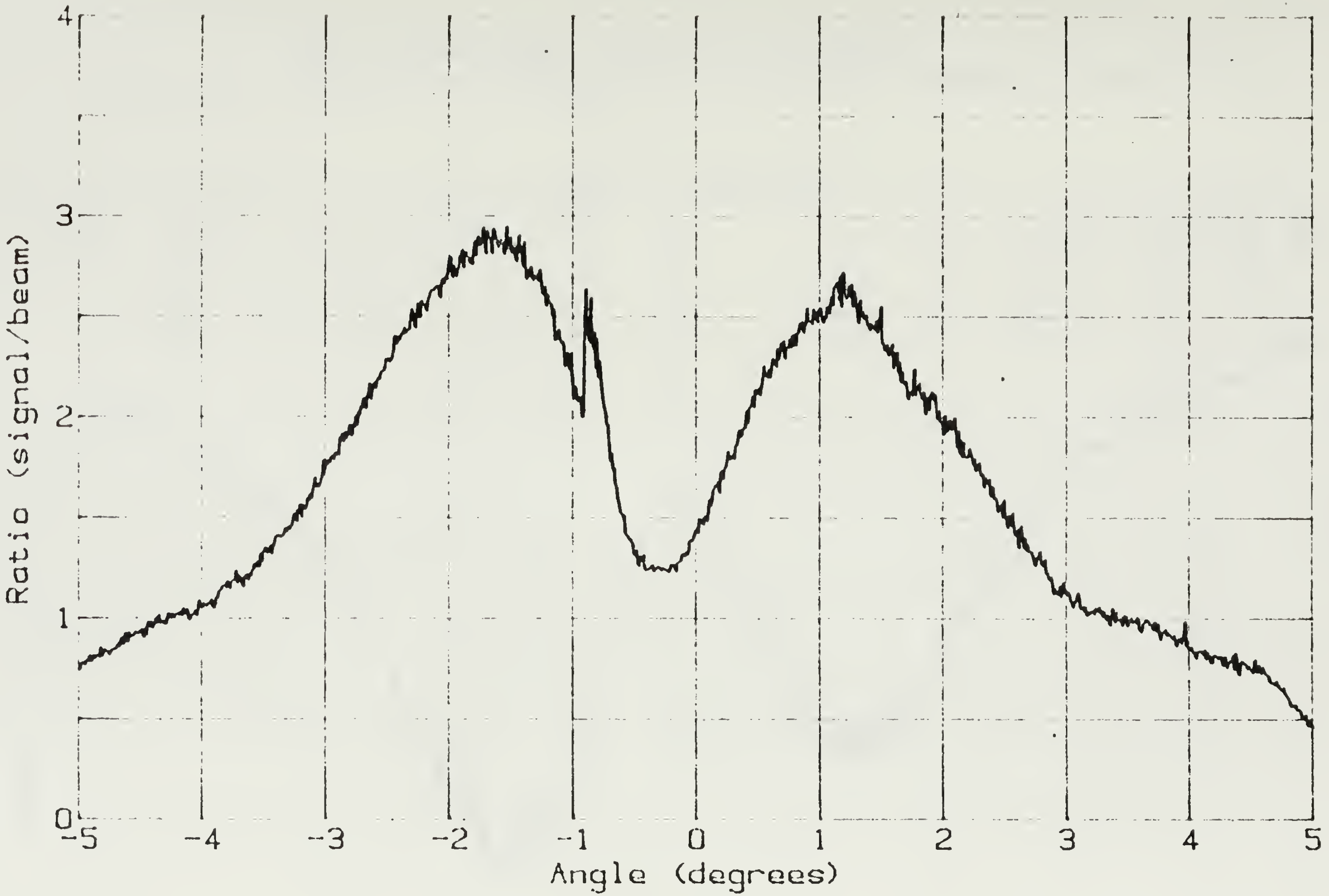

Figure 30. Normalized signal with a plastic tube without ends (Setup E, 63.3 MeV).

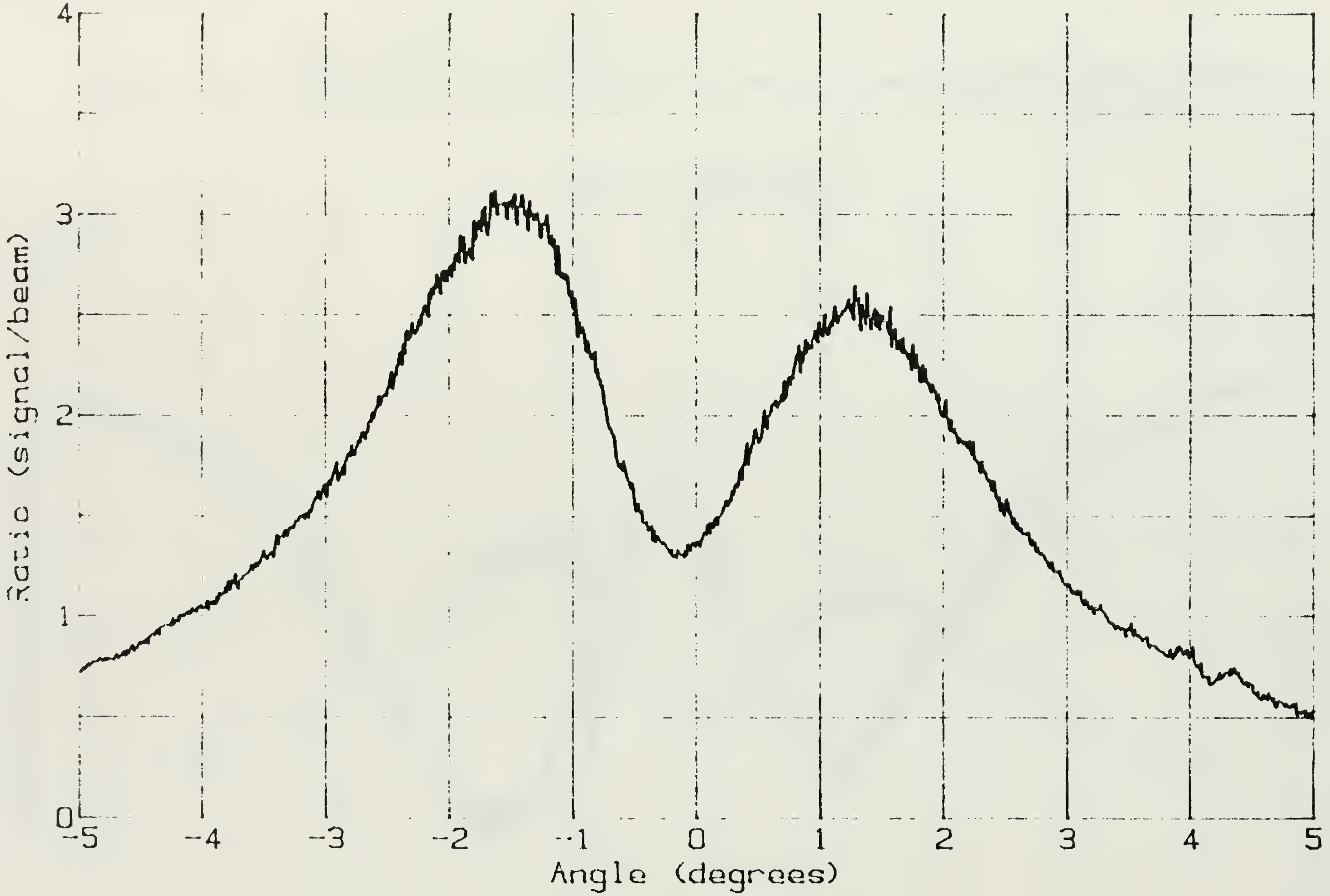

Figure 31. Normalized signal with no materials between the beam pipe and the detector (Setup F, 32.9 MeV).

TABLE 2

PEAK ANGLES

1. 32.9 MeV

Theoretical	Experimental	
	Setup	Peak angle
Cerenkov : 0.98^{0}	A - 7cm	1.3
	A - 5cm	1.3
	A - 3cm	1.4
	B	1.3
TR & DTR : 0.89^{0}	C	1.3
	D	1.8
	E	1.8
	F	1.8

2. 63.3 MeV

Theoretical	Experimental	
	Setup	Peak angle
Cerenkov : 1.24^{0}	A - 7cm	1.1
	A - 5cm	1.2
	A - 3cm	1.1
	B	1.2
TR & DTR : 0.46^{0}	C	1.1
	D	1.4
	E	1.4
	F	1.4

different as shown in Table 2. Since setups D, E, and F (see Figure 15) involve electron beam propagation in air, they mainly produce Cerenkov radiation and the peak is about at 1.8^0. On the other hand, setups A, B, and C (see Figure 15) removed most part of air and mostly produce DTR and TR. However, they should remove the effects of Cerenkov radiation. The observed experimental peak angle of these cases (setups A, B and C) is 1.3^0 and this angle is smaller than the peak angle of the experimental Cerenkov radiation (setups D, E and F). In the case of 63.3 MeV, the same result as the case of 32.9 MeV, the theoretical peak angle and the experimental peak angle for TR and DTR are both smaller than the peak angle of Cerenkov radiation as shown in Table 2. In both cases, there are large differences between theoretical peak angles and the experimental peak angles. It is suspected that the reason of this difference is the lack of an exact relationship for normalization, the incomplete elimination of other radiations, and the lack of the correct experimental boundary conditions incorporated in the theory.

Even though the height of the peak is theoretically decreased with increasing hole size, the experimental result of the effect of the hole size is very complicated. As shown in Table 3, the result of two energies is different and no sensible relation between the peak intensity and the hole size could be established. In the case of high energy,

TABLE 3.

HOLE SIZE EFFECTS

Hole Size (radius)	Peak			
	32.9 MeV		63.3 Mev	
	left	right	left	right
7 cm	2.2	2.0	2.2	1.8
5 cm	2.2	1.8	2.1	2.0
3 cm	2.5	2.6	2.1	2.7
0 cm (TR)	2.0	1.5	3.8	3.2

the intensity pattern looks like the theoretical prediction. But the other case (32.9 MeV) is very different. From Table 3, it is supposed that TR and DTR are more related to the theoretical prediction when the higher energy was used rather than the lower energy.

Comparing setup C and setup D, it is noticed that TR from the plastic bag is large when the higher energy electrons are used (Table 4). When comparing setup D and setup E, the peak value of two energies are different. This fact indicates again that TR and DTR from the plastic bag will be dependent on the beam energy. The intensity of setup F (only air between the beam pipe and the detector) is larger than setup E (just put plastic tube without ends). This tells about some amount of suppression due to the plastic tube.

TABLE 4.

PEAK OF EACH SETUP

Set up	32.9 MeV		63.3 Mev	
	left	right	left	right
C	1.6	1.3	3.4	2.5
D	1.3	1.3	1.3	1.1
E	1.2	1.1	2.8	2.5
F	1.6	1.4	3.0	2.5

B. CONCLUSIONS

Diffraction transition radiation was detected by direct measurement of radiation in these experiments. The X-band horn antenna passed through the beam path and found the first lobe of diffraction transition radiation, transition radiation, and Cerenkov radiation. It is found that the peak angle of TR and DTR is closer to zero degrees than the peak angle for Cerenkov radiation. Although these measured values are not the same as the theoretical values, the result show the same relation for both energies of 32.9 MeV and 63.3 MeV.

During these experiments, the relationship between the intensity of the signal and the hole size can not be found. But when the higher energy was used, it was easily found that increasing the hole size decreased the intensity of the signal.

Since the beam current is not constant, normalization is necessary to compensate for this beam fluctuation. But the rough assumption was made for the normalization due to the lack of the exact relation between the beam current and the signal. Digitization, which was achieved in these experiments, of the signal and the beam current has a lot of advantage for dealing with the data compared to the analog data. On the end of the beam pipe, all three radiations may be generated and these three radiations are detected all together at the antenna. In these experiments, the effort for separation of DTR was tried, but it was found that it is not enough. For a further experiment followings are recommended :

(1) Investigation of the higher beam energy using all three klystrons to find the relation between the beam energy and DTR.

(2) Find the exact relation of the signal to the beam current, and develop the arrangement of equipment for this purpose.

(3) Any meaningful efforts will require the isolation of DTR from the TR and Cerenkov radiation.

(4) More effort is needed to find out the relation between the hole size and the intensity of DTR.

(5) Reduction of the noise can improve the results.

APPENDIX A

LINAC CHARACTERISTICS

1.	Beam energy	15 MeV - 100 MeV
2.	Beam micro bunch length	0.0024 m
3.	Beam micro bunch distance	0.103 m
4.	Beam micro bunch charge	1.16×10^{-12} C
5.	Third harmonic frequency	8.568 GHz
6.	Third harmonic wavelength	3.5 cm

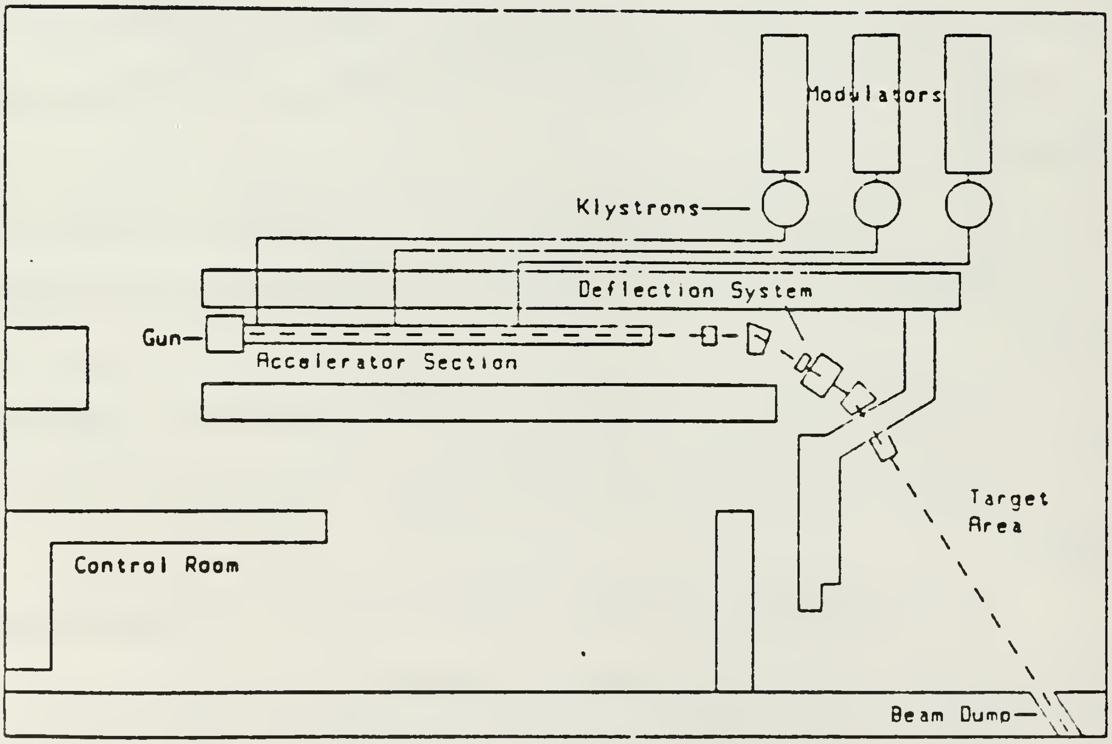

Figure 32. Experimental station

APPENDIX B

BASIC PROGRAM LISTINGS

1. Program for normalization

```
10     !This program provides a normalized radiation with a toroid
20     !on the beam pipe and moving horn antenna.
30     !Plotting is provided by HP 7090A.
40     !
50     !Main program
60     ASSIGN @Hp7090 TO 705
70     OPTION BASE 1
80     !
90     !Define the variables.
100    REAL Chan1(1:1000),Chan2(1:1000),Normal(1:1000)
110    INTEGER I,N,Factor
120    !
130    !Set initial conditions for the plotter.
140    OUTPUT @Hp7090;"RE13:"      !select channel 1 and 2 vs. time
150    OUTPUT @Hp7090;"IR10,10:"   !10 volts scale for each channel
160    OUTPUT @Hp7090;"TB18,0:"    !sets total time to 18 seconds
170    OUTPUT @Hp7090;"MS1:"       !sets buffered recording mode
180    !
190    !Takes data into buffers through 2 channels.
200    DISP "PRESS FILL BUFFER. IF FILLED, THEN PRESS CONTINUE,"
210    PAUSE
220    WAIT .5
230    !
240    !
250    !Subprogram command
260    GOSUB Data_trans
270    GOSUB Plot_area
280    GOSUB Plot_data
290    GOSUB Save_data
300    STOP
310    !
320
330    !Group of subprogram
340 Data_trans: !This subroutine takes data from 2 buffers
350             !and stores in array variables Chan1 and 2.
360             !
370             !Transfer channel 1 data to Chan1 array.
380                DISP "TRANSFERRING DATA"
390                OUTPUT @Hp7090;"DO1,1000,0,0:"
400                OUTPUT @Hp7090;"OI:"
```

```
410                FOR N=1 TO 1000
420                ENTER @Hp7090 USING "#,K";Chan1(N)
430                NEXT N
440             !
450             !Transfer channel 2 data to Chan2 array.
460                OUTPUT @Hp7090:"DD2,1000,0,0;"
470                OUTPUT @Hp7090:"OI;"
480                FOR N=1 TO 1000
490                ENTER @Hp7090 USING "#,K";Chan2(N)
500                NEXT N
510                RETURN
520             !
530             !
540 Plot_area:  !This subroutine draws the plotting area and grids.
550             !
560             !Define the plotting area
570                DISP "PLOT AREA IS DRAWING."
580                OUTPUT @Hp7090:"IP1700,1300,9800,6400;"
590                OUTPUT @Hp7090:"IW1700,1300,9800,6400;"
600             !
610             !Sets grid 10 for X-axis and 12 for Y-axis
620                OUTPUT @Hp7090:"GL10,12;"
630             !
640             !Select pen 4 and draw grid
650                OUTPUT @Hp7090:"SP4;DG0;"
660                RETURN
670             !
680             !
690 Plot_data:  !This subroutine plots the normalized transition
700             !
710                GOSUB Normal                        !normalize the data
720                DISP "NORMALIZED PATTERN IS DRAWING."
730             !
740             !Sets scale factor 1000, 1200 for X and Y-axis
750                OUTPUT @Hp7090:"SC0,1000,0,1200;"
760             !
770             !Select pen 3 and line type
780                OUTPUT @Hp7090:"SP3;LT;"
790             !
800             !Transfer normalized data from computer to plotter
810             !Set ratio 300% and drawing data
820                Factor=400                          !ratio (1200/3)
830                FOR N=1 TO 1000
840                IF N=1 THEN OUTPUT @Hp7090:"PUPA";N;Normal(N)*Factor
850                OUTPUT @Hp7090:"PDPA";N;Normal(N)*Factor
860                NEXT N
870                OUTPUT @Hp7090:"PU;SC;IW;"
880                DISP "PLOTTING IS COMPLETE."
890                RETURN
900             !
910             !
```

```
920 Normal:     !This program make a normalization for Chan1 and Chan2.
930             !Chan1 is a toroid and Chan2 is a moving antenna.
940             !
950               DISP "NORMALIZING TRANSITION PATTERN."
960               FOR I=1 TO 1000
970                 IF Chan1(I)=0 THEN            !avoid 0 value
980                   Chan1(I)=Chan1(I-1)
990                   Chan2(I)=Chan2(I-1)
1000                END IF
1010                Normal(I)=Chan2(I)/Chan1(I)
1020              NEXT I
1030              RETURN
1040            !
1050            !
1060 Save_data: !This subprogram save the data into separated file
1070            !which name is given by you.
1080            !
1090            !Save the beam data
1100              LINPUT "DO YOU WANT SAVE THE DATA ?",Answer$
1110              IF Answer$="N" THEN 1220
1120              LINPUT "ENTER FILE NAME TO STORE DATA: ",Name$
1130              MASS STORAGE IS ":,4,1"     !left drive as MSI
1140              CREATE BDAT Name$,3000,8    !3000 real numbers
1150              ASSIGN @Path TO Name$       !assign I/O path
1160              OUTPUT @Path;Chan1(*)       !send Chan1 data
1170              OUTPUT @Path;Chan2(*)       !send Chan2 data
1180              OUTPUT @Path;Normal(*)      !send Normal data
1190              ASSIGN @Path TO *           !close I/O path
1200              MASS STORAGE IS ":,4,0"     !return to right drive
1210              DISP "COMPLETE SAVING DATA."
1220              RETURN
1230
1240
1250 END
```

2. Program for redrawing of raw data

```
10    !This program is used to redraw the data in BDAT files.
20    !BDAT files store the data obtained using "NORMAL" program.
30
40    !Main program
50    ASSIGN @Hp7090 TO 705
60    OPTION BASE 1
70    !
80    !Define the variables
90    REAL Beam(1:1000),Signa(1:1000),Normal(1:1000)
100   !
```

```
110   !Subprogram command
120   GOSUB Load_data
130   GOSUB Plotting
140   DISP "PLOTTING IS COMPLETE."
150   STOP
160   !
170   !
180   !
190 Load_data:  !This program load the data from BDAT file
200             !into the program
210             !
220            !MASS STORAGE IS ":,4,1"        !left drive as MSI
230             LINPUT "ENTER A BDAT FILE NAME :",File$
240             DISP "TRANSFERING DATA FROM ";File$
250             ASSIGN @Path TO File$          !connect to file
260             ENTER @Path;Beam(*)            !load beam data
270             ENTER @Path;Signal(*)          !load signal data
280             ENTER @Path;Normal(*)          !load normal data
290             ASSIGN @Path TO *              !close the path
300            !MASS STORAGE IS ":,4,0"        !right drive as MSI
310             RETURN
320             !
330             !
340 Plotting:   !This program is for plotting with plotter.
350             !
360             !Choice the data to draw
370             PRINT "SELECT THE NUMBER TO DRAW."
380             PRINT "    1. BEAM & SIGNAL"
390             PRINT "    2. NORMALIZED SIGNAL"
400             !
410             INPUT "?",Choice
420             SELECT Choice
430             CASE =1
440                   GOSUB Plot_raw
450             CASE =2
460                   GOSUB Plot_normal
470             CASE ELSE
480                   BEEP
490                   PRINT "INVALID CHOISE."
500                   LINPUT "DO YOU WANT CONTINUE ?",Ans$
510                   IF Ans$="Y" THEN 370
520                   STOP
530             END SELECT
540             RETURN
550             !
560             !
570 Plot_raw:   !This subprogram plots the beam pattern.
580             !
590             DISP "BEAM PATTERN PLOTTING"
600             OUTPUT @Hp7090:"IP1750,2300,9250,7150;"
```

```
610               OUTPUT @Hp7090;"IZ1750,2300,9250,7150;"
620               OUTPUT @Hp7090;"SC0,1000,0,1000;"
630               OUTPUT @Hp7090;"SP1,LT2;"
640               FOR N=1 TO 1000
650                   IF N=1 THEN OUTPUT @Hp7090;"PUPA";N;Beam(N)*100
660                   OUTPUT @Hp7090;"PDPA";N;Beam(N)*100
670               NEXT N
680               OUTPUT @Hp7090;"PU;"
690               !
700               !
710               !This subprogram plots the detected signal.
720               OUTPUT @Hp7090;"SP2,LT;"
730               FOR N=1 TO 1000
740                   IF N=1 THEN OUTPUT @Hp7090;"PUPA";N;Signa(N)*100
750                   OUTPUT @Hp7090;"PDPA";N;Signa(N)*100
760               NEXT N
770               !
780               !Define drawing area, grid and pen
790               DISP "DRAWING PLOT AREA."
800               OUTPUT @Hp7090;"IP1750,2300,9250,7150;"
810               OUTPUT @Hp7090;"IZ1750,2300,9250,7150;"
820               OUTPUT @Hp7090;"GL10,10;"
830               OUTPUT @Hp7090;"SP4;DG0;"
840               OUTPUT @Hp7090;"PU;"
850               !
860               !Label X and Y axis.
870               DISP "LABELLING"
880               OUTPUT @Hp7090;"SI.2,.3;DI;"
890               FOR X=0 TO 1000 STEP 100
900                  OUTPUT @Hp7090;"PA";X;",0;"
910                  READ A
920                  OUTPUT @Hp7090 USING "#";"CP0,-.5;LO5;LB";A;""
930               NEXT X
940               DATA -5,-4,-3,-2,-1,0,1,2,3,4,5
950               OUTPUT @Hp7090;"PA500,-80;LBAngle (degrees)"
960               FOR Y=0 TO 1000 STEP 200
970                  OUTPUT @Hp7090;"PA0,";Y;";"
980                  OUTPUT @Hp7090;"CP-.5,0;LO8;LB";Y/100;""
990               NEXT Y
1000              OUTPUT @Hp7090;"SP1;PA-40,600;DI0,1;LT2;"
1010              OUTPUT @Hp7090;"LO5;LBBeam current  - - -"
1020              OUTPUT @Hp7090;"SP2;PA-60,600;DI0,1;LT;"
1030              OUTPUT @Hp7090;"LO5;LBRadiation     -----"
1040              RETURN
1050              !
1060              !
1070 Plot_normal:!This subprogram plots the normalized signal.
1080              !
1090              DISP "BEAM PATTERN PLOTTING"
1100              OUTPUT @Hp7090;"IP1750,2300,9250,7150;"
```

```
1110         OUTPUT @Hp7090;"IZ1750,2300,9250,7150;"
1120         OUTPUT @Hp7090;"SC0,1000,0,1200;"
1130         OUTPUT @Hp7090;"SP3,LT;"
1140         FOR N=1 TO 1000
1150             IF N=1 THEN OUTPUT @Hp7090;"PUPA";N;Normal(N)*300
1160             OUTPUT @Hp7090;"PDPA";N;Normal(N)*300
1170         NEXT N
1180         !
1190         !Define drawing area, grid and pen
1200         DISP "DRAWING PLOT AREA."
1210         OUTPUT @Hp7090;"IP1750,2300,9250,7150;"
1220         OUTPUT @Hp7090;"IZ1750,2300,9250,7150;"
1230         OUTPUT @Hp7090;"GL10,8;"
1240         OUTPUT @Hp7090;"SP4;DG0;"
1250         OUTPUT @Hp7090;"PU;"
1260         !
1270         !Label X and Y axis.
1280         DISP "LABELLING"
1290         OUTPUT @Hp7090;"SI.2,.3;DI;"
1300         FOR X=0 TO 1000 STEP 100
1310            OUTPUT @Hp7090;"PA";X;",0;"
1320            READ A
1330            OUTPUT @Hp7090 USING "K":"CP0,-.5;LO5:LB";A;""
1340         NEXT X
1350         DATA -5,-4,-3,-2,-1,0,1,2,3,4,5
1360         OUTPUT @Hp7090;"PA500,-80:LBAngle (degrees)"
1370         FOR Y=0 TO 1200 STEP 300
1380            OUTPUT @Hp7090;"PA1,";Y;";"
1390            OUTPUT @Hp7090;"CP-.5,0:LO8;LB";Y/300;""
1400         NEXT Y
1410         OUTPUT @Hp7090;"PA-50,500;DI0,1;
1420         OUTPUT @Hp7090;"LO5;LBRatio (signal/beam)"
1430         RETURN
1440         !
1450         !
1460 END
```

LIST OF REFERENCES

1. Rule, D.W. and Fiorito, R.B., Naval Surface Weapons Center Report Number NSWC TR 84-134, *The Use of Transition Radiation as a Diagnostic for Intense Beams*, July 1984.

2. Ter-Mikaelian, M.L., *High-Energy Electromagnetic Processes in Condensed Media*, Wiley-Interscience, 1972.

3. O'Grady, A.J., *Cerenkov Radiation, Transition Radiation and Diffraction Transition Radiation From Periodic Bunches For a Finite Beam Path In Air*, Master's Thesis, Naval Postgraduate School, Monterey, CA., June 1986

4. Gallet, M.J., *Diffrection Radiation From Relativistic Electron Bunches*, Master's thesis, Naval Postgraduate School, Monterey, CA., December 1986.

5. Buskirk, F.R. and Neighbours, J.R., *Cerenkov Radiation From Periodic Electron Bunches*, Physical Review A, Volume 28, Number 3, September 1983.

6. Buskirk, F.R. and Neighbours, J.R., Naval Postgraduate School, Report Number NPS-61-83-010, *Diffraction Effects in Cerenkov Radiation*, June 1983.

7. Bruce, R.G., *Cerenkov Radiation From Periodic Bunches For a Finite Path In Air*, Master's thesis, Naval Postgraduate School, Monterey, CA., June 1985.

INITIAL DISTRIBUTION LIST

		No. Copies
1.	Defense Technical Information Center Cameron Station Alexandria, Virginia 22305-6145	2
2.	Library, Code 0142 Naval Postgraduate School Monterey, CA 93943-5002	2
3.	Physics Library Code 61 Department of Physics Naval Postgraduate School Monterey, CA 93943-5000	2
4.	Professor F. R. Buskirk, Code 61Bs Department of Physics Naval Postgraduate School Monterey, CA 93943-5000	5
5.	Professor X. K. Maruyama, Code 61Mx Department of Physics Naval Postgraduate School Monterey, CA 93943	5
6.	Professor J. R. Neighbours, Code 61Nb Department of Physics Naval Postgraduate School Monterey, CA 93943-5000	2
7.	Library Korea Military Academy Gong-reung Dong 556-21 Seoul, The Republic of Korea 130-02	2
8.	Maj. Lee, Young Moon Ma-po Gu Yun-nam Dong 382-17 Seoul, The Republic of Korea 121-00	2
9.	Maj. Wee, Kyoum Bok SMC 2814 Naval Postgraduate School Monterey, CA 93943	1
10.	Maj. Yoon, Sang Il SMC 1558 Naval Postgraduate School Monterey, CA 93943	1
11.	Lt.Col. Jung, Yun Su Yong-deung-po Gu Yang-pyung Dong 4 Ga 27 Seoul, The Republic of Korea 150-00	1

12.	Maj. Kim, Jong Ryul SMC 1659 Naval Postgraduate School Monterey, CA 93943	1
13.	Cpt. Han, Hwang Jin SMC 2402 Naval Postgraduate School Monterey, CA 93943	1
14.	Mr. Donald S. Snyder, Code 61 Department of Physics Naval Postgraduate School Monterey, CA 93943-5000	1
15.	Maj. Youn, Duck Sang SMC 1254 Naval Postgraduate School Monterey, CA 93943	1
16.	Lt. W. Ftitchie PMW 145 SPAWAR Washington, DC 20363-5100	1
17.	Defense Advanced Research Project Agency ATTN: MAJ George P. Lasche 1400 Wilson Blvd. Arlington, VA 22209	1
18.	Dr. V. L. Granatstein Electrical Engineering Dept. University of Maryland College Park, MD 20742	1
19.	Lawrence Livermore National Laboratory University of California ATTN: Dr. William M. Fawley P. O. Box 808 Livermore, CA 94550	1
20.	Lawrence Livermore National Laboratory University of California ATTN: Dr. Ken Struve P. O. Box 808 Livermore, CA 93550	1
21.	Dr. Joseph Mack M4, M.S. P-940 Los Alamos National Laboratory Los Alamos, CA 87545	1
22.	Mission Research Corporation ATTN: Dr. N. J. Carron P.O. Box 719 Santa Barbara, CA 93102	

23. Naval Surface Weapons Center 1
White Oak Laboratory
ATTN: Dr. Han S. Uhm (R41)
10901 New Hampshire Avenue
Silver Springs, MD 20903-5000

24. Naval Surface Weapons Center 1
White Oak Laboratory
ATTN: Dr. Ralph Fiorito (R41)
10901 New Hampkshire Avenue
Silver Springs, MD 20903-5000

25. Naval Surface Weapons Center 1
White Oak Laboratory
ATTN: Dr. Donald Rule (R41)
10901 New Hampshire Avenue
Silver Springs, MD 20903-5000

26. CAPT. Kurt Stevens 1
AFTAC/TX OP
Patrick AFB
Patrick, FL 32925

27. MAJ. Edward Pogue
SD10-DE
Pentagon, Room 1E-800
Washington, DC 20301-7100

28. LCDR E. Turner 1
PMW 145
SPAWAR
Washington, DC 20363-5100

Thesis
L43565 Lee
c.1 Diffraction transition radiation from periodic electron bunches.

Thesis
L43565 Lee
c.1 Diffraction transition radiation from periodic electron bunches.

thesL43565
Diffraction transition radiation from pe
3 2768 000 78464 9
DUDLEY KNOX LIBRARY